



This is a repository copy of *Quantifying plant biology with fluorescent biosensors*.

White Rose Research Online URL for this paper:

<https://eprints.whiterose.ac.uk/225081/>

Version: Accepted Version

Article:

Rowe, J.H. orcid.org/0000-0002-3523-4347, Josse, M., Tang, B. et al. (1 more author) (2025) Quantifying plant biology with fluorescent biosensors. *Annual Review of Plant Biology*, 76. ISSN 1543-5008

<https://doi.org/10.1146/annurev-arplant-061824-090615>

© 2025 by the author(s). Except as otherwise noted, this author-accepted version of a journal article published in *Annual Review of Plant Biology* is made available via the University of Sheffield Research Publications and Copyright Policy under the terms of the Creative Commons Attribution 4.0 International License (CC-BY 4.0), which permits unrestricted use, distribution and reproduction in any medium, provided the original work is properly cited. To view a copy of this licence, visit <http://creativecommons.org/licenses/by/4.0/>

Reuse

This article is distributed under the terms of the Creative Commons Attribution (CC BY) licence. This licence allows you to distribute, remix, tweak, and build upon the work, even commercially, as long as you credit the authors for the original work. More information and the full terms of the licence here:

<https://creativecommons.org/licenses/>

Takedown

If you consider content in White Rose Research Online to be in breach of UK law, please notify us by emailing eprints@whiterose.ac.uk including the URL of the record and the reason for the withdrawal request.



eprints@whiterose.ac.uk
<https://eprints.whiterose.ac.uk/>

1 "Posted with permission from the Annual Review of Plant
2 Biology, Volume 76; copyright 2025 the author(s), <https://www.annualreviews.org>.

3 4 5 **Quantifying plant biology with fluorescent biosensors**

6
7 James H. Rowe*¹, Max Josse*¹, Bijun Tang*¹, Alexander M. Jones¹

8
9 *These authors contributed equally to this work

10 ¹Sainsbury Laboratory Cambridge University, Cambridge, United Kingdom

11
12 M.J.: <https://orcid.org/0000-0002-8444-5351> maxime.josse@slcu.cam.ac.uk

13 J.H.R.: <https://orcid.org/0000-0002-3523-4347>, james.rowe@sclu.cam.ac.uk

14 B.T.: <https://orcid.org/0000-0003-3689-0167>, Bijun.tang@slcu.cam.ac.uk

15 A.M.J.: <https://orcid.org/0000-0002-3662-2915>, alexander.jones@slcu.cam.ac.uk

16
17 Corresponding author: Alexander Jones, alexander.jones@slcu.cam.ac.uk

18
19 **Keywords:** (6 max) Genetically-encoded Fluorescence Biosensors, quantitative plant biology, live imaging,
20 molecular dynamics,

21
22 **Abstract:** (150 words max)

23
24 Plant biology is undergoing a spatial 'omics revolution, but these approaches are limited to snapshots of a
25 plant's state. Direct, genetically-encoded, fluorescent biosensors complement the 'omics approaches giving
26 researchers tools to assess energetic, metabolic, and signaling molecules at multiple scales, from fast
27 subcellular dynamics to organismal patterns in living plants. This review focuses on how biosensors
28 illuminate plant biology across these scales, and the major discoveries they have contributed towards. We
29 also discuss the core principles and common pitfalls affecting biosensor engineering, deployment, imaging
30 and analysis to help aspiring biosensor researchers. Innovative technologies are driving forward
31 developments both biological and technical with implications for synergizing biosensor research with other
32 approaches and expanding the scope of *in vivo* quantitative biology.
33
34
35
36
37

38 **Contents**

39 **INTRODUCTION 3**

40 **DISCOVERIES IN ENERGETICS, SIGNALING AND METABOLISM 4**

41 ENERGETICS 4

42 METABOLISM 4

43 SIGNALING 6

44 **DISCOVERIES IN DEVELOPMENT 7**

45 SYMBIOSIS AND NUTRIENTS 7

46 LIPIDS AND MEMBRANES 7

47 HORMONES 8

48 PH 9

49 CALCIUM (Ca²⁺) 9

50 **DISCOVERIES IN ENVIRONMENTAL RESPONSES & STRESS 10**

51 **CONCEPTS, CONSIDERATIONS AND CHALLENGES WHEN WORKING WITH BIOSENSORS 11**

52 BIOSENSOR ENGINEERING 11

53 BIOSENSOR DEPLOYMENT 13

54 BIOSENSOR IMAGING 13

55 BIOSENSOR IMAGE ANALYSIS 14

56 **CHALLENGES AND FUTURE DIRECTIONS 15**

57 **FIGURES 16**

58 **TERMS AND DEFINITIONS 22**

59 **REFERENCES ANNOTATIONS (UP TO 10, 20 WORDS EACH) 23**

60 **REFERENCES CITED 24**

61

62

63

64 Introduction

65 Plant biology is undergoing a spatial revolution. Single cell/nucleus transcriptomics (95, 138) and *in situ*
66 sequencing (94) provide maps of gene expression, and the trajectories of differentiating cells, sparking
67 debates and reassessment of what defines a cell type (133). Biotin ligases enable examination of the
68 subcellular proteome, through proximity-based labelling, allowing protein complexes to be characterized
69 (166), whilst fluorescence-activated cell sorting and laser capture microdissection proteomics are beginning
70 to offer cell type specific proteomes (33).

71 These methods produce big data with snapshots of a cell status, but without the context of other cellular
72 information *as well as responses to stimuli over time*, their application is limited. To understand how the
73 system is regulated we need to correlate single cell methods with the dynamics of key small molecules and
74 molecular events, whether they be metabolites, hormones, second messengers, reaction rates or post-
75 transcriptional modifications. These parameters may be transient, with information encoded in their spatial
76 or temporal dynamics. Fluorescent biosensors that are direct, specific, genetically-encoded and minimally-
77 invasive allow us to quantify these live cellular dynamics and provide synergistic information to cell and
78 sub-cellular gene and protein regulatory networks. Genetically encoded biosensors are not the only way to
79 approach questions of space and time in plant cells, and we encourage readers to seek out reviews on
80 fluorescent dye sensors, electrochemical biosensors, fluorescent ligands, turn-on molecules, spatially
81 resolved mass-spec, and endogenous fluorescent compounds (e.g. chlorophyll and coumarins) (59, 65, 75,
82 87, 88, 108, 112, 167, 174), which go beyond the scope of this review.

83 There are now far too many biosensors of differing mechanisms and analytes deployed in plants to
84 comprehensively summarize (see Table 1 and (63, 106, 134, 161)), so we have chosen a series of examples
85 to illustrate how they facilitate exciting biological discoveries at the (sub)cellular, organ, whole plant and
86 environmental context scales. This growing body of findings shows a maturing technology that is nonetheless
87 ripe for innovators and wider-adoption, and thus we also provide introductory views to biosensor
88 engineering, deployment, imaging and image analysis.

89 The palette of biosensors already engineered continues to grow, with rapid screening frameworks and high
90 throughput technologies used to engineer biosensors for diverse analytes (78). DNA synthesis technologies
91 combined with combinatorial cloning approaches allow sensor engineers to quickly screen multiple binding
92 domains, sensor conformations, and fluorescent protein variants, to isolate promising sensors. We discuss
93 these methods as well as the ongoing AI structural biology revolution (21, 23, 30, 80), which will also play an
94 important role in the development of future biosensors, allowing *in silico* predictions of potential sensor
95 structures and binding dynamics. The high throughput development of generalizable sensor designs, using
96 mutagenesis of well characterized protein scaffolds (16) or targeted development using nanobodies offer
97 promising opportunities for accelerated biosensor development. Combinatorial cloning techniques such as
98 Gateway (78) or Golden Gate (49) are also useful for biosensor deployment in plants, allowing engineers to
99 rapidly target a biosensor to several subcellular compartments or testing several promoter and terminator
100 combinations to minimize silencing of biosensor transgenes. But care must be taken to validate that the
101 biosensor will perform well in the chosen compartments, as many sensory domains and fluorescent proteins
102 are sensitive to variation in cellular conditions such as pH or oxidation.

103 Biosensors also have technical limitations for imaging and image analysis, the most obvious being optical.
104 Deep tissues are difficult to reliably and quantitatively image and autofluorescence may present a problem
105 in analysis, introducing artefacts that cloud interpretation. We discuss widely accessible solutions while also
106 highlighting advanced imaging techniques such as multiphoton microscopy that can help with imaging
107 deeper tissues and time-gated fluorescence imaging that can distinguish biosensor from auto-fluorescence.
108 Similarly, both highly accessible and advanced image analysis methods can improve the reliability of
109 biosensor image interpretation and allow users to extract vast amounts of meaningful data. For example,
110 automated segmentation separating objects and structures of interest permits focused quantification of
111 areas where the sensor is present thereby excluding artefacts from out of focus light and autofluorescence.

112 The primary focus of this review will be sensors which bind their analytes directly, thus altering their
113 fluorescent properties, and therefore do not require endogenous signaling components to function. These
114 direct biosensors can be targeted to different tissues and organelles and give high resolution spatial dynamics
115 of analyte changes, illuminating the subcellular differences in plant energy status(103) and the movement of
116 hormones between organs (132, 158). Biosensors can also be deployed to examine biotic interactions, such
117 as the flow of nutrients between symbionts (171), or how microbe induced nodules form (45). Biosensors
118 with fast binding and release kinetics also offer unparalleled temporal resolution, granting startling glimpses
119 of the information encoded in the signatures of second messengers like calcium (Ca^{2+}) (4, 163). These kinetics
120 offer another benefit. Quantitative readouts of analyte concentrations allow experimentalists to tease apart
121 biochemistry in living cells and organs, which can then inform and be cross-validated with modelling (129).
122 The ability to measure analytes directly allows modelers to overcome one of the main roadblocks in systems
123 biology, the difficulty of robust parameterization. Biosensors are therefore critical tools in understanding the
124 behavior at the system level. *Networked systems with complex inter-relationships* can be probed further with
125 sensors, as the wealth of plant biosensors means there are often sensors for multiple steps in a signaling
126 pathway, such as in stomatal regulation (72, 132, 158, 170).

127 The power of biosensors is self-evident, but they must also be put in their context. Just because an analyte
128 shows a spatial pattern or is changing under a given condition, how do we know which dynamics carry
129 meaningful information for the broader biological process? Traditional genetics, though informative, often
130 acts as a blunt tool with numerous pleiotropisms. To understand spatial and temporal responses, we also
131 need spatial and temporal tools. Using timed application of pharmacological inhibitors, inducible tissue
132 specific expression of enzymes/ signaling components (144) and tissue specific CRISPR (40) allows the
133 importance of analyte dynamics to be tested and validated at improved resolution. Emerging and future
134 precision perturbation technologies, most notably optogenetics (93, 120), are needed to fully exploit the
135 exquisite spatiotemporal resolution afforded by fluorescent biosensors and resolve primary functions from
136 secondary effects to more accurately build a coherent multiscale view of plant biology.

137 [Discoveries in energetics, signaling and metabolism](#)

138 Energetics, core metabolism, and signaling cascades are fundamental to life, with many of the same
139 molecular players shared across kingdoms. As autotrophs with organelles derived from ancestral
140 photosynthetic endosymbionts, the way that plants use these players can differ significantly with other taxa
141 such as animals or prokaryotes. Therefore, plant biologists have drawn from a large wealth of biosensors
142 for these core processes to take a quantitative lens to the multiscale and networked biological process of
143 energetics, signaling and metabolism.

144 [Discoveries in energetics, signaling and metabolism](#)

145 Bioenergetics, central metabolism, and signaling cascades are fundamental to life, with molecular players
146 shared across kingdoms. As autotrophs with organelles derived from ancestral photosynthetic
147 endosymbionts, the way that plants use these players can differ significantly from other taxa such as
148 animals or prokaryotes. Therefore, plant biologists have drawn from a wealth of biosensors for these core
149 processes to take a quantitative lens to the multiscale and networked biological process of energetics,
150 signaling and metabolism. At the same time the plant research community has been a major driver of their
151 development and application.

152 [Energetics and energy metabolism](#)

153 Decades before the first uses of GFP in plants, physiologists exploited endogenous fluorescent molecules to
154 understand dynamic photosynthetic responses. Photochemistry can be understood by exciting chlorophyll,
155 which dissipates excess energy as fluorescence, with a series of actinic and saturating light pulses (108). To
156 delve beyond the photosynthetic electron transport chain, into other aspects of energy metabolism, a suite
157 of engineered fluorescent biosensors have been used to decode the complexity of bioenergetics, where

158 reactions are compartmentalized across membranes and between organelles. Biosensors that bind or react
159 with their analyte directly can monitor rapid changes and be targeted to specific cellular compartments,
160 allowing bioenergetics to be studied *in situ*, rather than in isolated organelles, allowing the function of the
161 whole system to be characterized.

162 Adenosine triphosphate (ATP) is an essential energy source across kingdoms, and along with NADPH a main
163 product of the light reactions of photosynthesis. The ATeam AT1.03-nD/nA sensor which detects the
164 physiologically dominant $MgATP^{2-}$ form, shows large differences in the plant energy landscape under
165 different environmental conditions and between subcellular compartments and organs (37, 157). These
166 sensors allowed glimpses of the ATP: NADPH balance in the chloroplast stroma that is critical for
167 photosynthetic efficiency to be visualized in *Arabidopsis*. The light reactions and chloroplast ATPase cannot
168 supply enough ATP to completely support carbon fixation, so the ATP: NADPH ratio must be dynamic during
169 photosynthesis. Consequently, ATeam sensors confirmed *in vivo* that ATP in the chloroplast stroma
170 decreases as chloroplasts mature, but cytosolic ATP levels remained high, implying stromal ATP:NADPH is
171 not equilibrated in mature chloroplast stroma by ATP import (157). Instead, elegant use of the iNAP and
172 SoNar sensors (for NADPH concentration and NADH/NAD⁺ respectively) allowed visualization of the export
173 of reducing equivalents from chloroplasts, which support photorespiration in the mitochondria, with excess
174 reducing equivalents then exported to the cytosol through the Malate-OAA shuttle (103) resulting in
175 reduction of the NAD pool. Parallel work (48) demonstrated drastic changes in cellular pH during
176 photosynthesis, which cloud SoNar and iNAP interpretation, so used pH-resistant Peredox-mCherry sensors
177 to demonstrate NAD redox coordination across cellular compartments. iNAP and SoNar have now been
178 exploited to understand the origins of plastid ATP, NADPH and NADH for pollen tube elongation and
179 chloroplast ATP import for starch turnover to support stomatal opening (101, 104).

180 As well as exchanging metabolites, the mitochondria and chloroplast both send 'retrograde signals' to the
181 nucleus to respond to changing environmental conditions. This is essential as both the photosynthetic and
182 mitochondrial electron transport chains consist of a delicately balanced apparatus, sensitive to abiotic
183 stresses, such as high light, hypoxia, dehydration, or temperature. Comprehensive investigation of potential
184 mitochondrial retrograde signals, using a suite of sensors for $MgATP^{2-}$, H_2O_2 , NAD redox, pH, glutathione
185 reduction potential and Ca^{2+} strongly suggested that ROS is a likely cause of mitochondrial retrograde
186 signals (82).

187 Under chloroplast stress, H_2O_2 and E_{GSH} changes can be induced also in other compartments, including the
188 cytosol and the nucleus (153). Transient expression of the HyPer2 H_2O_2 sensor in *Nicotiana benthamiana*
189 pavement cells showed high-light induced chloroplastic, cytosolic and nuclear increases in hydrogen
190 peroxide (H_2O_2) (51). Strikingly, nuclear H_2O_2 persisted when a cytosol-targeted ascorbate peroxidase (APX)
191 is overexpressed, but not when APX was targeted to the stroma. As many chloroplasts touch the nucleus,
192 this implies H_2O_2 movement through plastid-nuclear complexes or stromules to coordinate high-light
193 responsive nuclear gene expression (51). For both the chloroplast and mitochondria, targeted biosensor
194 localization has allowed the field to uncover the movement of H_2O_2 signals between compartments to alter
195 gene expression, insights that could only be obtained by studying the signals in their cellular and
196 subcellular context. Recent developments of pH resistant sensors (102, 119, 136, 154), and more specific
197 H_2O_2 sensors (52) will continue to push this field forward.

198 Metabolism

199 Alongside energetics, biosensors have illuminated the world of sugar metabolism and nutrient allocation. A
200 concerted effort to engineer an array of biosensors for metabolites (41, 53, 89, 135) means that plant
201 biologists have a host of powerful tools to draw upon. A sensitivity series of glucose sensors were used to
202 demonstrate considerable variation in glucose levels between tissues, with roots showing lower glucose
203 levels than leaf epidermal and guard cells (41). FLIPsuc sucrose sensors derived from *Agrobacterium* sugar
204 binding proteins (89) were used to screen libraries of membrane proteins to discover the Sugars Will
205 Eventually Be Exported Transporter (SWEET) family of sucrose transporters (28). SWEET transporters are

206 conserved across kingdoms and in plants they are key for unloading sugars from source cells and tissues
207 (28). Later, these SWEET transporters were used to build transport sensors, enabling direct measurement
208 of glucose transport activity through AtSWEET1 and allowing the authors to build a quantitative model of
209 AtSWEET1 function. This model could be used to calculate rate constants for shifts between conformations
210 during sugar export (123).

211 Plant survival is also limited by uptake of nutrients brought up from the soil, particularly macronutrients
212 fixed nitrogen, inorganic phosphate and potassium (K^+). Various nutrient sensors have been specifically
213 engineered for plants. Ammonium transport-activity sensor Amtrac1 was first developed to understand
214 ammonium uptake and showed that rather than passive gas channels, ammonium transporters show
215 dynamic changes of conformation during transport, for which the sensor gives a measurable readout (9,
216 38). Similarly, transceptor-based sensors for nitrate transport give an output that replicates the dual affinity
217 uptake kinetics of the CHL1/NRT1.1 protein (71). Although potentially useful to understand structural
218 functional dynamics in heterologous and homologous systems, transporter-based sensors are
219 complementary to direct analyte sensors as they reflect the activity transporter, rather than linking
220 fluorescence output with *in vivo* analyte concentrations. Recently, a FRET-based sensor for nitrate
221 (NitraMeter3.0) has been developed and deployed in *Arabidopsis* roots, which detects distinct nitrate levels
222 in different cell files and locally different accumulation dynamics in response to nitrate treatment (29).

223 An improved version of the inorganic phosphate sensor FLIPPi (68), cpFLIPPi has been deployed in plants,
224 showing different phosphate levels between organs and organelles (118). Targeting FLIPPi to chloroplasts
225 shows complex phosphate dynamics modulated by transporters and photosynthesis in different leaf
226 tissues, as well as limitations that phosphate insufficiency imposes on photosynthesis (127). Recently,
227 sensors for the last major macronutrient, K^+ have been engineered and deployed in *Arabidopsis* and tested
228 with salt stress, demonstrating a potassium efflux to counterbalance sodium influx and prevent membrane
229 depolarization, as well as the interplay between K^+ , Ca^{2+} and ROS in roots (162, 165).

230 Signaling

231 Although biosensors have been used to study an array of signaling pathways in diverse biological contexts,
232 they have perhaps been exploited best in the study of stomata. Infrared gas analysis and epidermal peel
233 bioassays have allowed stomatal aperture to be studied in context or isolated from other tissues, but in
234 both cases biosensors allow the study of the fast complex signaling networks underlying stomatal
235 dynamics. The array of biosensors available for H_2O_2 , Ca^{2+} , Abscisic acid, Glutamate, CPK activity and SnRK2
236 activity have successfully been deployed to help elucidate the complex signaling networks underlying
237 stomatal dynamics (4, 72, 100, 125, 132, 158, 170).

238 Early work using the Yellow Cameleon (YC2.1) calcium sensors demonstrated transient Ca^{2+} spikes following
239 stomatal closure stimuli, such as ABA or CO_2 , but only in subpopulations of cells (5, 168). Temporal
240 dynamics of Ca^{2+} responses are often critical to elicit specific responses (163). The ABA responsive OST1
241 kinase can directly phosphorylate important ion channels for stomatal closure such as SLAC1, but work with
242 R-GECO1-mTurquoise clearly demonstrates that the ABA-induced Ca^{2+} transients enhance closure (72).
243 Inducing Ca^{2+} transients with exchanges of hyperpolarizing and depolarizing buffers, validated with YC2.1,
244 allowed researchers to decode the specific timing of Ca^{2+} transients for maximum stomatal closure (4). This
245 work also demonstrated the importance of CALCIUM DEPENDENT PROTEIN KINASE 23 (CPK23) for ABA and
246 Ca^{2+} dependent closure dynamics (4).

247 Why ABA or CO_2 only induce measurable Ca^{2+} transients in a subpopulation of stomata remains a mystery.
248 However in the case of ABA, the Ca^{2+} transients are partially ROS and RBOH dependent, potentially
249 indicating a system gated by multiple signals (86). ABA and CO_2 induced Ca^{2+} transients were consistent
250 with a priming model, where CO_2 or ABA can prime Ca^{2+} receptors for activation (168). In addition to
251 CPK23, recent work has shown an interaction between CPK21 and ABA repressed ABI1 phosphatase as
252 another point of ABA- Ca^{2+} crosstalk. ABI1 inhibits the activity of CPK21, which can be relieved by ABA to

allow CPK21 to activate the anion channel SLAH3 and promote closure (60). Recently, sensors for the activity of CPK21 and CPK23 were developed, demonstrating how their different affinities for Ca^{2+} allow distinct signal processing in stomata and other tissues such as root hairs (100).

Rather than a single pathway, the CPK, Ca^{2+} and ABA work indicates that stomatal signaling relies on a complex network of quantitative signaling events that are integrated to give an opening or closure response. This has echoed in investigation of the role of ABA in CO_2 signaling. Although ABA biosynthesis and signaling mutants may display sluggish or absent closure responses to CO_2 (26), the ABALEON2.15 and SNACS sensors showed no stomatal ABA accumulations or OST1 signaling in short term CO_2 treatments (170). This implies that a basal level of ABA signaling is required for stomatal CO_2 closure responses and high levels of ABA amplify the CO_2 closure responses.

Signaling is complex and at any given moment, a plant must respond to not one environmental signal, but must integrate the responses to a vast array of inputs, some of which may necessitate conflicting responses. Biosensors allow stomatal biologists to test these interconnected networks in a reduced two cell system. However biosensors also allow researchers to examine signaling on the tissue to organ scale and study the complex control of developmental biology, as discussed in the next section.

Discoveries in Development

Symbiosis and Nutrients

As for stomata, the plant cells involved in symbiotic interactions with microorganisms (e.g. rhizobia bacteria and arbuscular mycorrhizal fungi (AMF)) undergo a complex set of signaling as they coordinate specialized nutrient physiology and the formation of symbiotic organs or structures. The use of direct biosensors in legume model plants, especially *Lotus japonicus* and *Medicago truncatula* has revealed the specific hallmarks of nodulation symbiosis, and the importance of nuclear Ca^{2+} spiking to both. The **YFP-aequorin** and **YC2.1** Ca^{2+} sensors decoded Ca^{2+} responses in *Lotus japonicus* roots used to distinguish between symbiotic or pathogenic fungal responses (17). Although nuclear Ca^{2+} spiking is essential for nodulation, the source of the Ca^{2+} dynamics was unclear until Ca^{2+} biosensors were deployed. YC2.1 showed that rhizobia induce DMI1- and MCA8-mediated Ca^{2+} dynamics at the nuclear periphery in *Medicago*, indicating Ca^{2+} release from the nuclear envelope connected to the ER (24) and **NRCG-GECO1** (a two-color sensor for nuclear and cytoplasmic Ca^{2+} responses) demonstrated that the nuclear Ca^{2+} spiking preceded the cytosolic oscillation (83) indicating a non-cytosolic-adjacent source. Recent work using the GA biosensor **nlsGPS2**, showed that endogenous bioactive GA is low in primary and lateral roots and accumulates early in nodule development and persists in the nodule apex, acting as a positive regulator of nodule growth and development (45). Nodule development features a unique GA accumulation signature that was found to be regulated by organ-identity transcription factors, likely because of increased GA biosynthesis (45).

In AMF symbiosis, the inorganic phosphate (Pi) sensor, **cpFLIPPi**, was used to monitor cytosolic and plastidic Pi level in *Brachypodium distachyon* mycorrhizal root cells. By tracing Pi flux in AMF colonized cortical cells in responses to extracellular Pi, differential direction and magnitude of cytosolic Pi were demonstrated to depend on cell type and arbuscule status (171).

Lipids and membranes

The amphipathic nature of anionic phospholipids such as phosphatidic acid (PA), phosphatidylserine (PS), and phosphatidylinositol-phosphate (PIP) is fundamental for membrane bilayers and cellular life. Genetically encoded fluorescent lipid biosensors have demonstrated functional lipid gradients and dynamics at the subcellular level. The development of multi-affinity '**PIpline**' markers enabled the study of plant PIPs in a

297 variety of tissues and developmental contexts. PIP, PA, and PS are separately required to generate the
298 electrostatic signature of the plant PM and their specific accumulation patterns in different compartments
299 of the cell determine organelle identity (124, 145, 146). For example, **cYFP-2xPH^{PLC}** imaging demonstrated
300 that highly electronegative domains form via accumulation of PI4P, contributing to the PM localization and
301 function of several proteins involved in hormone and receptor-like kinase signaling (146). Using inducible
302 PI(4,5)P₂ depletion system revealed PI(4,5)P₂ dynamics between PM/cytosol is involved in lipid-mediated
303 intracellular signaling and root hair elongation, root growth and organ initiation in *Arabidopsis thaliana* (44).
304 Biosensors for PI(4,5)P₂ and PI4P (**mCitrine-P4M^{SidM}** and **mCitrine-PH^{PLC}**), at the shoot apical meristem
305 showed a correlation between mechanical stress, cortical microtubules and PI(4,5)P₂ accumulation,
306 suggesting that PIP4 specific accumulation patterns determine local cell behaviors underlying organ
307 development (147).

308 The **GFP-N160_{RbohD}** biosensor for PA dynamics shows that gravity stimulation results in asymmetric PA
309 distribution at the root apex due to differential activity of Phospholipase-D (98), complementing previous
310 work showing that sphingolipids mediate Phospholipase-C-driven consumption of PI4P at the Trans-Golgi
311 network (TGN) rather than local PI4P synthesis, which is important for the polar sorting of the auxin
312 transporter PIN2 at the TGN (74). Live-imaging of PI4P and PI(4,5)P₂ biosensors (**2xCherry-PH^{FAPP1}** and **mCIT-
313 2xPH^{PLC}**) in micro-fluidics grown *Arabidopsis* root hairs was used to show that pharmacological inhibition of
314 PIK5P3 activity, a major enzyme converting PI4P to PI(4,5)P₂, alters PI4P/PI(4,5)P₂ dynamics between the
315 apical plasma membrane and endomembranes resulting in root hair cell growth arrest (142). That PI4 kinase
316 activity appears essential at the plasma membrane suggests that root hair growth depends on cytoplasmic
317 streaming (142).

318 Hormones

319 Auxin (indole-3-acetic acid, IAA) is a master coordinator of cell proliferation, elongation and differentiation
320 throughout the plant's life cycle and mediates nearly all developmental processes. Therefore, the
321 (sub)cellular dynamics of IAA have been a core focus of plant research for decades (34) leading to the
322 development of multiple reporter systems. The most common and accessible IAA reporters, **DR5** and **DR5v2**,
323 are synthetic auxin responsive promoters driving the expression of reporters such as GUS, luciferase or
324 fluorescent proteins. DR5 reports a subset of the transcriptional auxin output and has been widely used to
325 spatially characterize auxin-mediated developmental processes in diverse plant species (76, 99, 155). **DII-
326 VENUS** and **R2D2** are nuclear-localized, degron-based auxin signaling sensors, in which DII-VENUS is
327 degraded by the proteasome in presence of IAA (19, 99). A key limitation of both DR5 and DII/R2D2 for
328 quantification of auxin is reliance on the endogenous nuclear auxin signaling machinery that is largely
329 nuclear, so they cannot be targeted to other cellular compartments. They also offer limited temporal
330 resolution and slow reversibility as observing rapid auxin depletion relies on protein synthesis and
331 fluorophore maturation (for DII) or fluorophore turnover (for DR5). Recently the first direct, FRET-based auxin
332 sensor, **AuxSen** (70), was reengineered from the bacterial FLIP-W tryptophan sensor (81). AuxSen allows
333 direct, reversible visualization of exogenous auxin at the subcellular level (nuclear or endoplasmic reticulum),
334 but it has micromolar affinity ($K_{d_{IAA}} > 1 \mu\text{M}$) that is likely to miss important endogenous auxin dynamics
335 thought to occur in the nM range (11). However, other FRET-based sensors have been successfully developed
336 to monitor endogenous dynamics of the plant hormones abscisic acid (ABA) and gibberellins (GA).

337 **ABACUS1** biosensors could detect reversible and dose-dependent ABA accumulation following exogenous
338 ABA pulses in roots growing using the RootChip, and **ABAleon2.1** tracked the long-distance translocation of
339 ABA from the shoot to the roots (78, 158). High-affinity and high SNR **nlsABACUS2** sensors were used to
340 investigate endogenous ABA dynamics in both shoot and roots under stress. By combining sensor imaging
341 with light sheet microscopy and high-resolution genetic perturbations, the authors demonstrated that shoot
342 to root ABA transport through the phloem and unloaded in root tips was vital for roots to continue growing
343 at low relative humidity (132). ABACUS2 also demonstrated that xerobranching, the developmental response
344 inhibiting lateral root formation when roots lose contact with water, is regulated by radial movement of the
345 stele-derived ABA. This ABA disrupts intercellular communication between inner and outer cell layers

346 through plasmodesmatal closure resulting in (105) blocked inward movement of auxin, visualized with DR5
347 and DII-VENUS, and inhibited lateral root formation (111). In addition to root development, ABACUS2
348 biosensors in combination with ABA transporter knockdowns for *ABCG17* and *ABCG18* showed that these
349 ABA transporters are required for proper ABA distribution during seed development (173). *ABCG17/18*
350 knockdowns had high ABA in the valve, septum, funiculus and outer seed tissues but lower ABA levels in the
351 embryos and this resulted in larger seeds.

352 The gibberellin biosensor **nlsGPS1** was used to discover endogenous GA gradients in dark-grown Arabidopsis
353 hypocotyls of wild-type and light-signaling mutants and primary root tips (130). Combining mathematical
354 modelling with high-resolution GA measurements using **nlsGPS1**, the authors then dissected the biochemical
355 basis for GA gradients in Arabidopsis roots (129). Combining mathematical models of hormone homeostasis
356 with experimental measurements will establish a new framework for future simulations of hormone
357 dynamics, which are tightly regulated through biosynthesis, catabolism and transport, within organs with
358 distinct growth zones. The more reversible and orthogonal **nlsGPS2** GA biosensors show that the key
359 determinant of the GA gradient in dark-grown hypocotyls is COP1 signaling gating expression of the
360 biosynthetic enzyme *GA20ox1*, whereas PIFs are required to maintain but not to establish GA gradients and
361 HY5 represses GA accumulation in the hypocotyl during photomorphogenesis (66).

362 pH

363 While typically acting as a positive growth regulator in the shoot, auxin accumulation represses root
364 elongation, leading to a long-standing enigma of how the same molecule can have opposite roles depending
365 on context. The rise of direct sensors allowing live quantification of small molecules and ions has provided
366 unprecedented clues to resolve this mystery, which relates to the Acid Growth Theory where lowering of the
367 apoplast pH directs cell elongation (69). In the shoot, the genetically-encoded apoplastic pH sensor **Apo-**
368 **pHusion** was combined with pharmacological and genetic manipulations to show that auxin-induced
369 activation of the plasma membrane H⁺-ATPases leads to apoplast acidification and thus promotes shoot
370 growth (55).

371 In contrast, root Apo-pHusion imaging revealed apoplastic alkalinization in elongation zone cells upon auxin
372 treatment, suggesting IAA-driven H⁺ influx (62). This observation was complemented by **pH_{cyto-PM}** reporter
373 for intracellular pH which showed ultra-fast (<1min) decrease in plasma membrane adjacent cytosolic pH of
374 elongation zone cells after treatment with 5 nM IAA (97, 107). The rapid IAA-mediated root growth inhibition
375 is concomitant with apoplastic pH increase and intracellular pH decrease, but also rapid Ca²⁺ transients
376 detected using **GCaMP3** (150) in the elongation zone (97). Li et al., elegantly demonstrated that in the root,
377 TMK1- and TIR1/AFB-based signaling machineries act antagonistically towards apoplast acidification to
378 regulate auxin-mediated root growth (97). These observations are consistent results from the **Acidins2/3/4**
379 low-pH sensors which showed a differential alkalinization between the inner and outer face of the
380 Arabidopsis root tip under gravistimulation (pH 5.35 versus pH 5.2)(116). This strongly supports a link
381 between auxin depletion, decreased apoplastic pH, cell wall acidification and increased root cell elongation
382 (13).

383 Although the links are not clearly established, those mechanisms of rapid pH change driving root cell
384 elongation are accompanied by auxin-mediated CNGC14 activity with rapid Ca²⁺ spikes acting as a second
385 messenger Ca²⁺ influx has been shown to be accompanied by pH changes in Arabidopsis root tip (141, 160).

386 Calcium (Ca²⁺)

387 Ca²⁺ signatures shape many aspects of plant development, including pollen tube development, root
388 hydrotropism, and root hair growth (18, 57, 143, 149, 172). Ca²⁺ oscillations often depend on the activity
389 plant cyclic-nucleotide-gated channels CNGCs. Using **YC3.6** and **R-GECO1** cytosolic Ca²⁺ sensors, Gao et al.,
390 demonstrated that Ca²⁺ channels CNGC18 is essential for pollen tube guidance in Arabidopsis (57); while
391 Zhang et al., showed that loss-of-function *cngc14* is sufficient to cause hairless roots when grown on standard

392 agar media (172), consistent with other reports that CNGC-mediated oscillatory Ca^{2+} gradients in the root
393 hair tip are essential for growth and polarity in *Arabidopsis* (18, 149). The knockdown of CNGC14 channel
394 had previously been reported to abolish cytosolic Ca^{2+} signaling in gravistimulated roots, while wild-type
395 plants exhibit a rapid auxin-induced elevation of cytosolic Ca^{2+} levels (141). Later studies support the link
396 between auxin perception, and Ca^{2+} -mediated root development, both in root hairs and primary root. Dindas
397 et al. and Waadt et al., independently reported that local auxin application induces immediate inwardly
398 directed proton fluxes and bi-phasic spikes of cytosolic Ca^{2+} (as measured with **R-GECO1**) requiring CNGC14
399 and functional TIR1/AFB-Aux/IAA pathway (43, 160). However, auxin-induced spikes occur within seconds so
400 must result from a TIR1/AFB-Aux/IAA non-transcriptional signaling output, as suggested by the similar rapid
401 TIR1/AFB-Aux/IAA-dependent auxin-induced inhibition of *Arabidopsis* root growth (54).

402 The targeting of **NRCG-GECO1.2** to the cytoplasm and nucleus demonstrates functional nuclear Ca^{2+} spikes
403 in *Arabidopsis*, while genetic disruption of nuclear membrane-localized ion channels DMI1 and CNGC15 is
404 sufficient to alter primary root development including meristem development and auxin homeostasis (DII-
405 VENUS signals) echoing the mechanisms controlling calcium spiking during rhizobial symbiosis (96). These
406 findings are of interest since TIR1/AFB was recently discovered to include a guanylate cyclase catalytic
407 domain involved in rapid Ca^{2+} oscillations induced by auxin. Live-imaging of **GCaMP3** sensors showed an
408 increase cytosolic Ca^{2+} spikes after application of cGMP (126). cGMP production is rapidly stimulated by auxin
409 and is involved in the rapid Ca^{2+} oscillations and root growth inhibition, demonstrating that cGMP is an
410 important second messenger in the auxin response with CNGC14 as a likely downstream target (126). This
411 study exemplifies how biosensor imaging can be used to link developmental observations and the molecular
412 mechanisms involved, expanding our understanding of non-transcriptional TIR1/AFB activity.

413 Discoveries in Environmental Responses & Stress

414 One of the great promises of direct fluorescent biosensors is the ability to spatially resolve stress responses
415 as they happen and therefore reveal the quantitative dynamics that transmit information during signal
416 transduction. To maximize insight from such fluorescence measurements, one must recreate the stress in an
417 imaging modality compatible with the target biosensors. A classic example of multiscale information flow
418 during stress responses involves ABA translocation from roots to leaves during water stress to effect stomatal
419 closure and limit water loss (77). However, more recent studies suggested that leaves were key sources of
420 ABA biosynthesis following perception of peptide, sulfate or hydraulic signals from water stressed roots or
421 locally experienced aerial humidity stress (77). The use of indirect or destructive methods revealed that ABA
422 can move shoot to root to effect growth stimulation and alter root-shoot ratios (109) while direct ABA
423 biosensors (ABAlcons and ABACUS) permitted the non-destructive analysis of shoot to root ABA translocation
424 in living *Arabidopsis* plants (77). Recently, Rowe et al. established an endogenous function for shoot to root
425 ABA in maintaining primary root elongation during a humidity stress (132). This study demonstrates the
426 utility of direct biosensing to quantify the timing, cell-type and sub-cellular locale of growth stimulatory ABA
427 concentrations in roots. Local osmotic stress including high salinity is another condition where ABA dynamics
428 are known to be important. While a series of indirect ABA reporters have provided insight into local ABA
429 dynamics in salt stressed roots (46, 164), nlsABACUS2 imaging revealed a more quantitative view of nuclear
430 ABA accumulations crucial for reprogramming roots for growth under stress (132).

431
432 Another advantage of quantitative biosensor analyses during stress responses is the ability to examine the
433 spatiotemporal interrelationships between multiple signals, for example in the biosensing of long-distance
434 Ca^{2+} waves travelling at 0.4mm/sec initiated by salt stress (32). These waves were found to be partially
435 dependent on ROS generation by NADPH oxidase (RBOH) (152) and could be quantitatively compared with
436 RBOH dependent ROS waves previously visualized with fluorescent dyes that were also initiated by salt stress
437 and travelled at 1.4mm/sec (113). In the case of systemic signaling following wounding, an abiotic stress that
438 also informs herbivory signaling, the use of Ca^{2+} (e.g. GECOs, GCaMPs, MatryoshCaMP6s, YC3.6), ROS (roGFP,
439 HyPer, roGFP-Orp1, HyPer7) and extracellular glutamate sensors (e.g. iGluSnFR) biosensors has greatly
440 expanded upon early studies examining the spatiotemporal dynamics of the aforementioned ROS waves
441 (113) as well as electrical potential waves (117). Today it is clear that a series of signals are mobilized to

442 rapidly transmit, relay and/or sense long-distance stress signals in plants, including electrical potentials, ROS,
443 Ca^{2+} , glutamate or other amino acids (131, 134), pH (139), mobile proteins (58), and hydraulic pressure
444 changes sensed at membranes (64, 115). These signals and their interactions have further been shown to
445 involve a series of genetic components using quantitative imaging of biosensors in mutant backgrounds
446 including, for example extracellular glutamate and pH sensitive Ca^{2+} channels, vacuolar Ca^{2+} channels,
447 hyperosmolality-gated Ca^{2+} -permeable channels, cyclic nucleotide-gated ion channels, plasma membrane
448 ROS generating enzymes, proton-pumps and stretch-activated Ca^{2+} channels (GLRs, TPC1, OSCA1, CNGCs,
449 RBOH, AHA1, MSL10,(50, 113, 115, 117, 139, 151, 169). Recently, green leaf volatiles were shown to induce
450 Ca^{2+} signaling, quantifying the potential for plant wound signaling, along with associated defense priming, to
451 extend to neighboring individuals or species (8). Notably, with concurrent and quantitative contributions
452 from a series of signals, biosensor imaging data must be interpreted in light of potential impacts on the
453 biosensor on the signaling events (110), for example the expression of FLIPE^{surface} FRET biosensors for
454 glutamate led to developmental defects indicating that extracellular glutamate signaling may be important
455 for more than just wound and stress signaling (25). Furthermore, it is important to consider possible crosstalk
456 among signals where biosensors may exhibit cross-reactivity (e.g. glutamate and Ca^{2+} sensors showing pH
457 sensitivity).

458
459 Much like abiotic stresses, plant immune response under biotic stress is a multifaceted process involving
460 early signaling events, such as change of intracellular Ca^{2+} levels and rapid increase of ROS (i.e. oxidative
461 burst) as well as transcriptional reprogramming of hormone pathways mediated by salicylic acid, jasmonic
462 acid and ethylene. The coincidence and crosstalk between key players (Ca^{2+} , ROS and hormone signaling) at
463 varying times and sub-cellular locations during biotic stress parallels plant wounding responses, but immune
464 responses have received comparatively less attention in biosensor imaging. Nonetheless, examples using
465 HyPer and roGFP2-Orp1 ROS biosensors demonstrate the value of tracking the spatiotemporal dynamics of
466 an oxidative burst triggered by flg22, a pathogen-associated molecular pattern, treatment (119) and mito-
467 roGFP line was used to investigate the role of mitochondria in ROS accumulations during pathogen
468 responses(56). As improved biosensors become available regularly, there is great potential to apply them to
469 quantify such responses more accurately and specifically as recently accomplished for flg22 ROS responses
470 using HyPer7 (154). Ca^{2+} responses to flg22 have also been investigated with biosensors to investigate
471 molecular players involved in signaling (e.g. CNGCs) (151) and to probe the spatial patterns of Ca^{2+} responses
472 over different organs and over time . Direct biosensing of defense phytohormones awaits development of
473 SA, JA and ethylene sensors, but already the potential for insight is clear from indirect spatial analysis of
474 promoter-reporters or degron-sensors during pathogen or herbivore attack (e.g. SA responsive PR1:GUS (22)
475 and JA-Ile responsive Jas9-Venus (92). In the disease triangle of plant disease, not only the plant responses
476 but also the pest or pathogen and environment play crucial roles, and therefore, the quantitative information
477 at high spatiotemporal resolution provided by minimally-invasive direct biosensors could be particularly
478 useful. For example, nlsABACUS2 was recently utilized in during herbivory responses to resolve the
479 relationship of ABA accumulation and stomatal defense against spider mite infestation (131).

480 Concepts, considerations and challenges when working with biosensors

481 Biosensor Engineering

482 A central challenge when engineering a novel biosensor protein is that the number of biosensor designs it is
483 possible to screen for activity is dwarfed by the combinatorial sequence space of sensory domain, fluorescent
484 protein and linker variants. Nonetheless, experience can guide aspiring biosensor engineers to the most
485 promising variants and screening methodologies to bias for success. First and foremost is selection of sensory
486 domains – often responsive to signaling events or ligand binding without requiring other cellular components
487 - with appropriate properties to the eventual use cases envisioned (e.g. matched dynamic range of detection,
488 reversibility, and compatibility with the organisms, cells, or sub-cellular compartments of interest). The
489 molecular events underpinning sensory domains can range from simple binding in the case of intrinsic ligand-
490 sensitive fluorescent proteins and domains that change conformation upon ligand binding (79, 122), to more
491 complex in the case of transport activity sensors or sensory domains engineered to change conformation

492 upon a signaling event such as phosphorylation (Figure 1). Sensory domains relying on molecular events or
493 machinery external to the biosensor itself such as those in translocation and degradation-based signaling
494 sensors (e.g. gibberellin signaling sensors based on DELLA protein degradation (7, 140) can provide
495 complementary information to direct analyte biosensors (e.g. Gibberellin Perception Sensors GPS1 and GPS2
496 (66, 130) in the same pathway as signal transduction is sensitive to the abundance of upstream signals as
497 well as receptors and downstream signal transduction components. In lieu of direct biosensing, signaling
498 sensors and transcriptional reporters can provide useful indirect views on upstream signals (e.g. DR5 and
499 DR5v2 promoter-FP reporters (99, 155) and DII-VENUS based (20) signaling sensors for auxin) until direct
500 biosensors can be engineered and deployed (see AuxSen discussion below). However, indirect methods are
501 less quantitative and increasing the number of molecular events involved increases susceptibility to artefacts
502 from non-specific dynamics of external components or crosstalk from other signals. Therefore, unless the
503 downstream signaling event is the chief interest, e.g. for FRET-based kinase sensors that report on ABA-
504 dependent phosphorylation (170), choice of sensory domain should emphasize the simplest form that is
505 proportional to the target molecule or molecular event.

506 After determination of the sensory domain, the fluorescent protein outputs should also be well matched to
507 future applications for properties like brightness, photostability, maturation rate and pH sensitivity.
508 Depending on the number of fluorescent proteins, the sensor can be intensimetric when the signal is
509 quantified by a single fluorescence emission, or ratiometric when the signal involves comparison to a control
510 emission. Generally, intensimetric imaging is easier to employ, analyze and multiplex and can have high
511 signal-to-noise ratio whilst ratiometric imaging is less susceptible to expression and depth of imaging
512 artefacts and can thus be more quantitative. In multi-fluorophore sensors that rely on fluorescent resonance
513 energy transfer (FRET), spectral overlap between donor emission and acceptor excitation should be
514 maximized while donor and acceptor bleed-through should be minimized (121). Other than classic FRET
515 pairs, ratiometric biosensors can be constructed using circularly permuted FP (cpFPs) with control FPs - most
516 elegantly in Matryoshka biosensors (10, 47) - or make use of bioluminescence resonance energy transfer
517 (BRET). Addition of a separate control fluorescent protein on the same transcript (via P2A ribosomal skipping
518 sequence) or a separate expression cassette can aid ratiometric quantification of otherwise intensimetric
519 degron-based sensors, translocation sensors, and transcriptional reporters (12).

520 Finally, connecting linkers or insertion sites for the individual components must be selected and optimized
521 to increase the dynamic range of response. Improving signal-to-noise ratio (SNR), which is related to the
522 amount of signal change observed relative to baseline noise, is application dependent but is the biggest
523 factors to consider when engineering the dynamic range of biosensor response. Commonly, altering the
524 length and flexibility of the sequences in or adjacent to the sensory domain-fluorescent protein (SD-FP)
525 linkers is the most efficient way to optimize initial biosensor designs that exhibit good sensory properties
526 such as affinity and reversibility but have low dynamic range of fluorescence response (e.g. small cpFP
527 intensity change or low FRET ratio change (161).

528 To complete the design-build-test cycle for biosensor engineering, cloning platform and testing system are
529 equally essential for improving throughput. While 2-part combinatorial assembly using Gateway has proved
530 valuable for engineering FRET biosensors (FRET pairs with sensory domains) (29, 71, 78, 84, 130), multi-part
531 combinatorial assembly of genetic parts using Gibson or Golden Gate assembly are flexible and efficient
532 methods for rapid construction of biosensor designs. Common expression systems for biosensor engineering
533 include rapid heterologous systems (i.e. *Escherichia coli* or protease deficient *Saccharomyces cerevisiae*) as
534 well as transient plant expression systems benefiting from more realistic target environments (i.e. protoplasts
535 or *Nicotiana benthamiana* leaves). Testing biosensor variants can make use of emerging high-throughput
536 directed evolution methods like ratiometric FACS (105) with ligand treatments or arrayed nanodroplets, but
537 has thus far relied primarily on lower throughput methods(85). An efficient design-build-test cycle helps to
538 screen through more candidates to improve sensory properties and increase the dynamic range of sensor
539 response. Following initial screens, it is common for biosensor optimization to iterate through rounds of
540 mutation and careful biochemical characterization of affinity, reversibility, pH sensitivity and specificity. For
541 example, the evolution of genetically encoded calcium indicators over the past 25 years involved several

542 crucial steps to improve their signal-to-noise ratio to expand detection dynamics range (2, 108). Today there
543 are numerous successful biosensors engineered for plant biology (e.g. sensors for key sugars, phytonutrients
544 and phytohormones discussed below) and many successful applications in plants of sensors originally
545 developed for other systems (e.g. sensors for metabolites, second messengers, and ions) showing that direct
546 biosensors are highly transferrable parts.

547 Biosensor deployment

548 There are many potential applications of a novel biosensor beyond direct expression in plant cells (Figure 2).
549 Direct sensors offer a viable alternative to HPLC-MS for quantifying agonists and antagonists *in vitro* using
550 purified sensor (128), whereas biosensors can also be employed as screening tools in a high-throughput
551 heterologous system. For example, an endoplasmic reticulum (ER) FRET-based glucose sensor (148) was
552 employed to identify AtSWEET1, a transmembrane glucose transporter belonging to the novel SWEET family,
553 in the HEK293T (human embryonic kidney) cell system (27). Nonetheless, a key advantage of biosensors lies
554 in their capability to provide spatial and temporal resolution of ligand distribution within living systems. Often
555 the first applications are in transient systems (e.g. *N. benthamiana* leaves, protoplasts or legume hairy roots)
556 or stable transgenics in *Arabidopsis thaliana*. But biosensors can be used in any species or organ where the
557 analyte is relevant, particularly when *Arabidopsis* is an insufficient host as for a series of symbiosis studies
558 discussed below.

559 Upon initial deployment in the target plant cell or species, it is often necessary to further fine-tune, diversify
560 or re-engineer next-generation biosensors. Potential problems range from lack of expression, gene silencing,
561 unmatched affinity or insufficient SNR or orthogonality. Weak or absent fluorescence in certain cells or
562 tissues, often caused by silencing or incompletely constitutive promoter-terminator combinations, has been
563 observed repeatedly, for example the Ca²⁺ sensor Cameleon expressed only in guard cells (6), glucose and
564 ABA sensors showing transgene silencing prompting analysis in silencing mutant *rdr6* (42) and HyPer showing
565 silencing especially beyond their seedling stage (15). Utilizing multiple combinations of promoters and
566 terminators and screening through large populations of transgenic events can significantly improve biosensor
567 expression level and SNR even for biosensors that initially show severe silencing (130, 132). Once expressed,
568 it is important to validate the biosensor or ideally an affinity series (132) of biosensors for high SNR detection
569 of the physiologically relevant range of the sensing target in the target tissues. Optimally, this would involve
570 a full *in vivo* titration to calibrate the biosensor response in plants with *in vitro* kinetic data (91), but more
571 often calibration can make use of mutants or tissues with low levels treated to progressively increase the
572 sensing target (130). It is also important to gauge orthogonality (66) *in vivo* by examining host plant
573 phenotypes for hyper- or hypo-sensitivity to the sensing target which is evidence that the sensor is
574 interfering with endogenous signaling. To detect possible interference from endogenous signaling with
575 biosensor outputs (i.e. artefactual or non-specific dynamics), low-affinity or entirely non-responsive (NR)
576 variants can be deployed as negative controls. Often it is possible to use biosensors with imperfect SNR,
577 specificity, affinity or orthogonality in compatible use cases whilst awaiting or re-engineering next-
578 generation biosensors. For example, an *Arabidopsis* nlsGPS1 line is hyposensitive to GA₄ and this phenotype
579 issue was resolved by inverting charges at two electrostatic interactions in the sensory domain to generate
580 GPS2 that maintains biosensor response but does not cause hyposensitivity in an *Arabidopsis* nlsGPS2 line
581 (66, 130). Rapid expansion of genome sequences and high-resolution protein structures provides valuable
582 information for this fine-tuning of biosensor properties while emerging artificial intelligence tools (1, 80)
583 may eventually enable design or re-design of biosensors *in silico*.

584 Biosensor imaging

585 There are several technical reviews focused on live-imaging plant tissues (35), therefore we will focus on
586 discussing the core principles, common pitfalls and limitations of plant biosensor imaging. Quantifying
587 plant biology through the lens of biosensors is often a tradeoff between spatial and temporal resolution.
588 Spatial resolution can be affected by the sensor's attributes (brightness, cellular localization, and
589 expression pattern), the sample features (thickness, autofluorescence), and the imaging equipment
590 (resolution, magnification, etc.). Similarly, temporal resolution is dependent on the sensor (e.g. dynamic

591 range, reversibility, maturation time) and the imaging setup and equipment (sample survivability, image
592 acquisition time).

593 Among the most common pitfalls inherent to biosensor imaging, light scattering and plant-specific
594 autofluorescence are particularly problematic. Although the emergence of 2-photon microscopy (2PM) and
595 fluorescent lifetime imaging (FLIM) techniques offer ways to image deeper or overcome tissue
596 autofluorescence, equipment availability is a problem and FLIM requires complex image acquisition,
597 processing and analysis.

598 Biosensor imaging setups must compromise between acquisition speed, resolution, and signal-to-noise
599 ratio and compromise on signal strength and channel saturation. For ratiometric sensors (e.g. FRET
600 sensors), it is especially important to use matched detectors and keep a consistent detector gain between
601 the two channels. Combining sensitive detection equipment such as GaAsP or HyD detectors, or CCD
602 cameras, saving data at the highest supported bitrate (most detectors are 12- or 16-bit, but default to 8-bit
603 output to save space) will offer the best signal to noise ratio. Laser power should be high enough to allow
604 quantitative imaging, but low enough to minimize photobleaching, particularly for timecourses.

605 Co-expression of pairs of direct biosensors for multiparameter analyses has opened new possibilities (159,
606 160), however it requires careful consideration of microscope settings. When imaging multiple sensors
607 (multiplexing) or adding a dye into your imaging setup, it is necessary to consider the spectral overlaps,
608 which can result in fluorescence bleed-through and artefacts.

609 While manageable for single FP sensors, using ratiometric sensors may limit the choices of usable dyes
610 (e.g. no blue, yellow or green dyes with CFP/YFP FRET-sensors); tools such as FPbase spectra viewer
611 (<https://www.fpbase.org/spectra/>) allow optimized imaging setups when using multiple laser
612 channels/dyes (90). The future development of homo-FRET biosensors would allow easier multiplexing, as
613 they only emit at a single wavelength. Most FRET biosensors are based on CFP-YFP variants and need ~425-
614 448nm light sources to excite CFP without exciting YFP rather than the 405 and 458nm lasers most
615 commonly available. A general rule should be for users to check is they have adequate lasers for the sensor
616 they plan to use. Finally, quantifying plant biology with biosensors requires using correct controls, often a
617 non-responsive sensor variant harboring mutation abolishing sensory domain/ligand binding. The local
618 cellular environment (pH, oxidation, other detectable analytes) is another point to consider when imaging
619 biosensors, since those can influence function of the sensors (YFPs are notoriously sensitive to pH due to
620 high pKa, and circularly permuted FPs are easily oxidized).

622 Biosensor image analysis

623 It is easy to underestimate the difficulty of creating fast robust image analysis workflows and the quantitative
624 power that they provide. Comprehensive analysis suites such as FIJI (137), python/napari (31), Icy (36),
625 IMARIS and MorphographX (39) allow users to create flexible workflows, that can be supplemented with
626 user written plugins or automated for batch analysis.

627 Image analysis can broadly be broken down into three key steps, preprocessing, segmentation and
628 quantification, with the optional steps of registration and tracking (**Figure 4**).

629 Preprocessing steps involve preparing the image for subsequent analysis steps, for example removing noise
630 and background subtraction may make both the segmentation and quantification steps more robust (**Figure**
631 **4A**). Performing image registration (**Figure 4B**), which involves finding the same objects or features between
632 images allows multiview acquisitions to be combined or allows the translation of timecourses to negate
633 sample movement artefacts for downstream analysis.

634 The segmentation step divides the image into different areas to be analyzed separately, which can be
635 performed manually (e.g. with manually drawn regions of interest in FIJI), or automated through software
636 (**Figure 4C**). Semantic segmentation, where each pixel is classified as either 'sensor' or 'not sensor' can be
637 achieved by techniques including intensity-based thresholding, which involves using software to mask only
638 parts of the image where intensity is above or below a threshold value. This also prevents interpreting pixels
639 where the biosensor fluorescence is absent/low or the detector is saturated, either of which could introduce
640 artefacts and compromise interpretation (**Figure 4D**). Instance segmentation, where each instance of an
641 object (e.g. organelle, cell or plant) is labeled separately, allows more detailed and nuanced biological
642 questions to be asked. Good instance segmentation can pay dividends in the quantification step, allowing

643 biosensor output to correlated with other morphological and spatial characteristics, for example cell size or
644 shape (**Figure 4D**). Furthermore, combining instance segmentation with object tracking allows biosensor
645 outputs from individual cells to be tracked through time. During quantification, calibrated absolute
646 quantification is the gold standard, but often requires more information than is available. Ratiometric, or
647 normalized quantification can control for many artefacts, such as local brightness or expression differences.
648 Raw intensimetric quantification methods are susceptible to artefacts but can offer excellent dynamic
649 range and SNR.

652 Challenges and Future Directions

653 The broader context for the expansion in development and application of genetically-encoded fluorescent
654 biosensor is an increasing recognition that biology will need more quantitative and higher-resolution
655 datasets in order to progress from mechanistic understanding of molecular functions to systems level
656 understanding of multiscale and networked biological processes. Biosensor research in plants is faced with
657 a number of difficult challenges, from mismatched biosensor biochemical properties to slow deployment or
658 imaging difficulties in the target subcellular compartment, cell, organ or species of interest. Each of these
659 challenges can be overcome, with the future outlook becoming ever more promising due to concurrent
660 technical advances accelerating protein engineering, plant transformation, live imaging application to
661 larger, deeper and more autofluorescent tissues, and pipeline development for automated image analysis.
662 Already plant scientists have produced captivating and quantitative views of complex biological processes
663 unfolding in vivo. To quantitatively answer a specific biological question, biosensors are often used with
664 uniquely tailored imaging experiments and analysis pipelines. To promote the broader use of biosensors by
665 the community and to facilitate the training of the next generation of quantitative plant biologists, imaging
666 setups, scripts, algorithms, computational tools, etc., need to be carefully informed and broadly
667 distributed. Much of the current zeitgeist is linked with probing crosstalk among networked components,
668 often with multiplexed sensing or unravelling the signal integration upstream and program activation
669 downstream of cellular analyte dynamics using higher-resolution genetic perturbations and multiscale
670 mathematical modelling. Certainly, there is value in minimally-invasive analyses and getting cell and
671 subcellular information in the context of a living plant, but quantification is only the beginning as the
672 specific genesis and function of each dynamic can be targeted for interrogation. When considering the
673 single-cell revolution in 'omics' technologies, including high-resolution metabolomics, unlocking synergies
674 between these datasets and biosensor imaging data will be potent next steps.

676 Acknowledgements

677 Many thanks to Alex Costa and Markus Schwarzländer for helpful comments on the manuscript. We
678 gratefully acknowledge funding from the Gatsby Charitable Foundation.

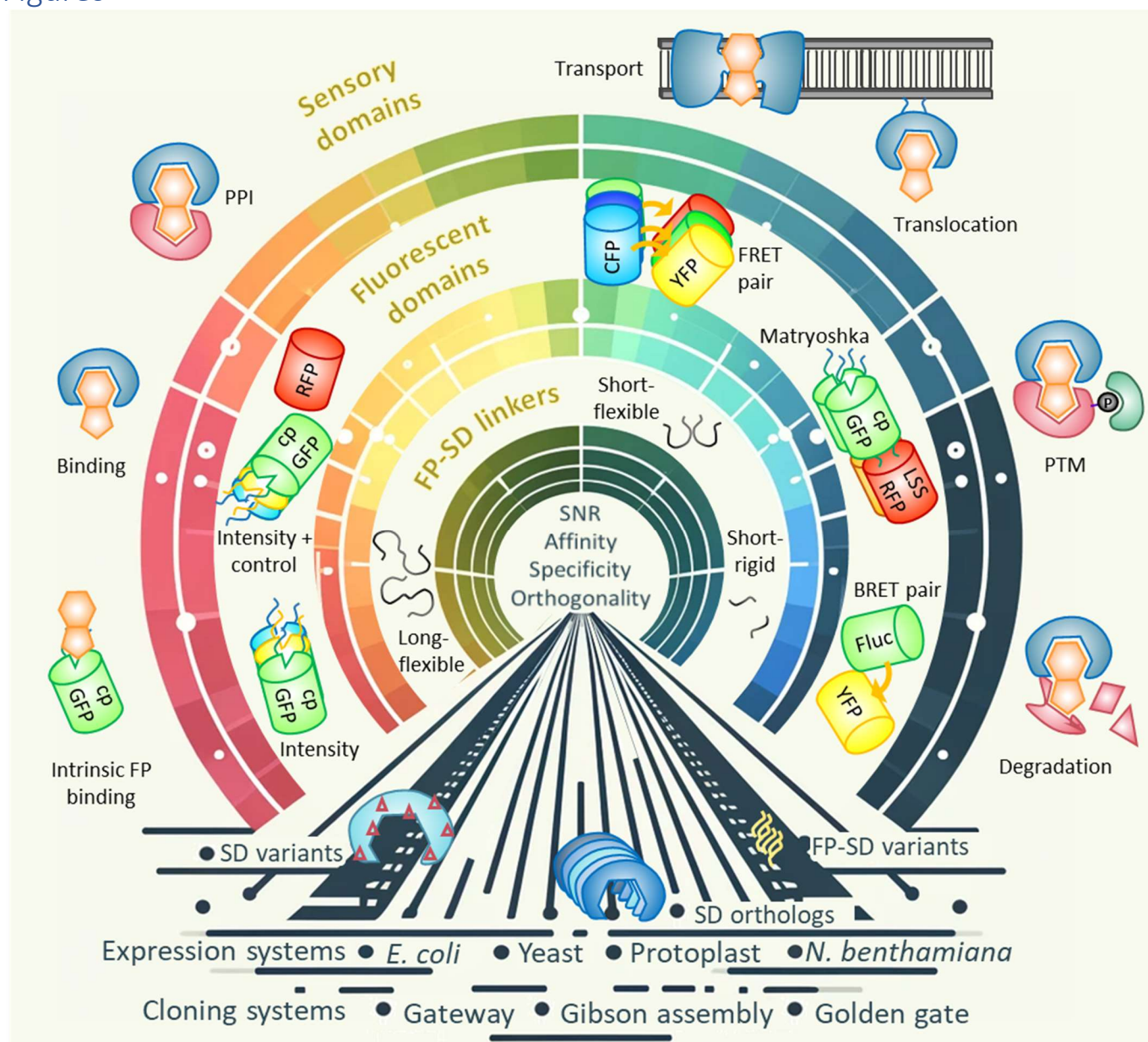
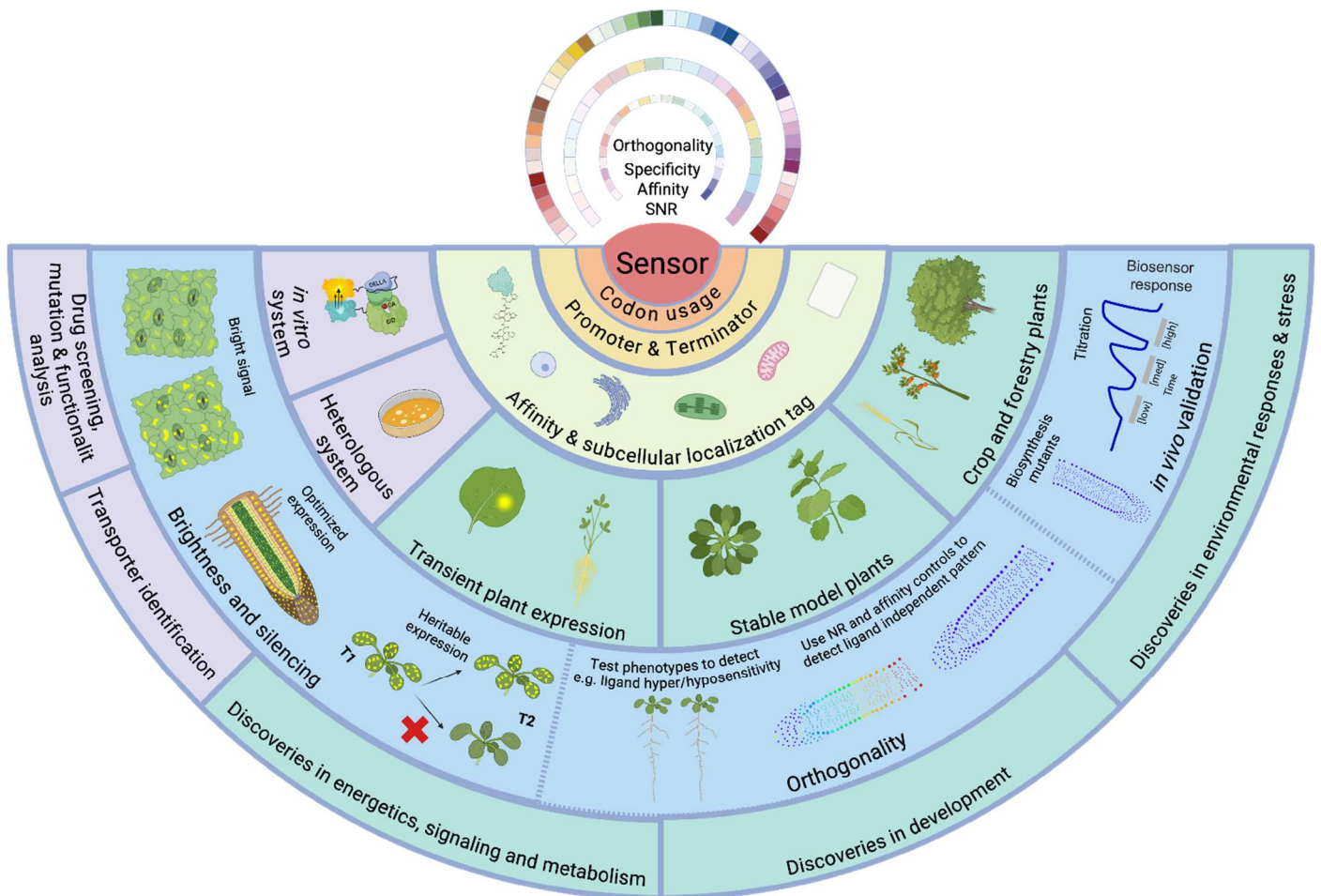
680
681

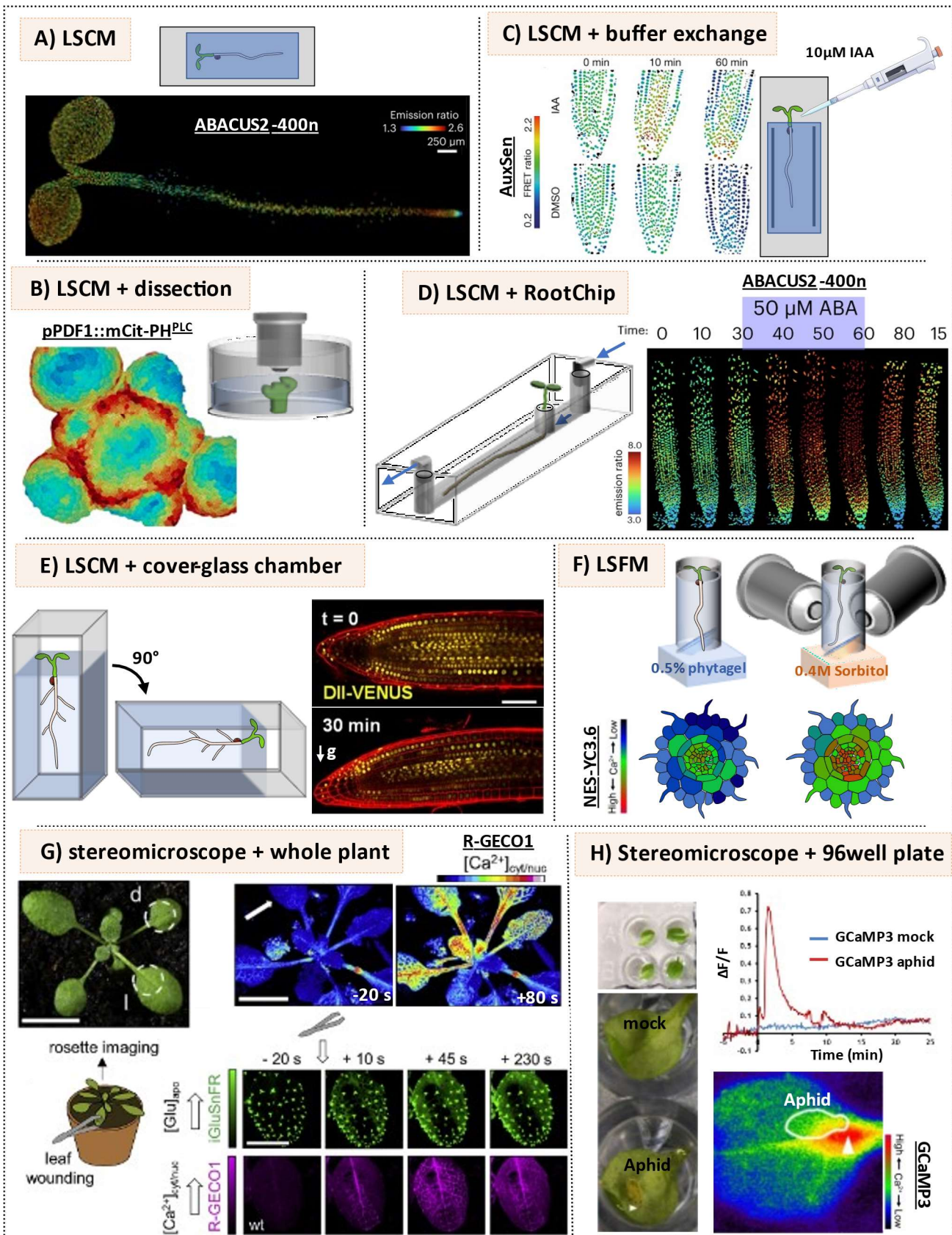
Figure 1. The path to engineering a fluorescent biosensor. Engineering of a novel genetically-encoded fluorescent biosensor begins with selection of a sensory domain or domains that are dynamic in proportion to the biological process of interest (e.g. conformation, translocation or abundance). Next a fluorescent domain or domains are selected from a series of types with intensity-based outputs often offering ease of use and higher signal-to-noise ratio and ratiometric outputs (e.g. FRET or Matryoshka) offering quantitative results less susceptible to imaging or expression level artefacts. Among the many sequences available to fuse fluorescent proteins with sensory domains (FP-SD linkers), short linkers with a proline residue are often preferred and are compatible with Gibson assembly and Golden-gate cloning strategies. The design-build-test cycle of biosensor engineering requires a high-throughput expression system ranging from *E. coli* being fastest and *N. benthamiana* transient expression being biologically closest to application conditions. The pipeline from initial sensor design to one optimized for orthogonality, specificity, affinity and signal-to-noise ratio is non-linear. Screening sensory domain orthologs to find appropriate orthogonality, specificity and affinity can be followed with rational or unbiased mutagenesis to further optimize or diversify these parameters. Any part of the biosensor can be re-engineered to improve signal-to-noise ratio, including changing fluorescent proteins, but a common successful target is focused mutation at the FP-SD linkers.

696



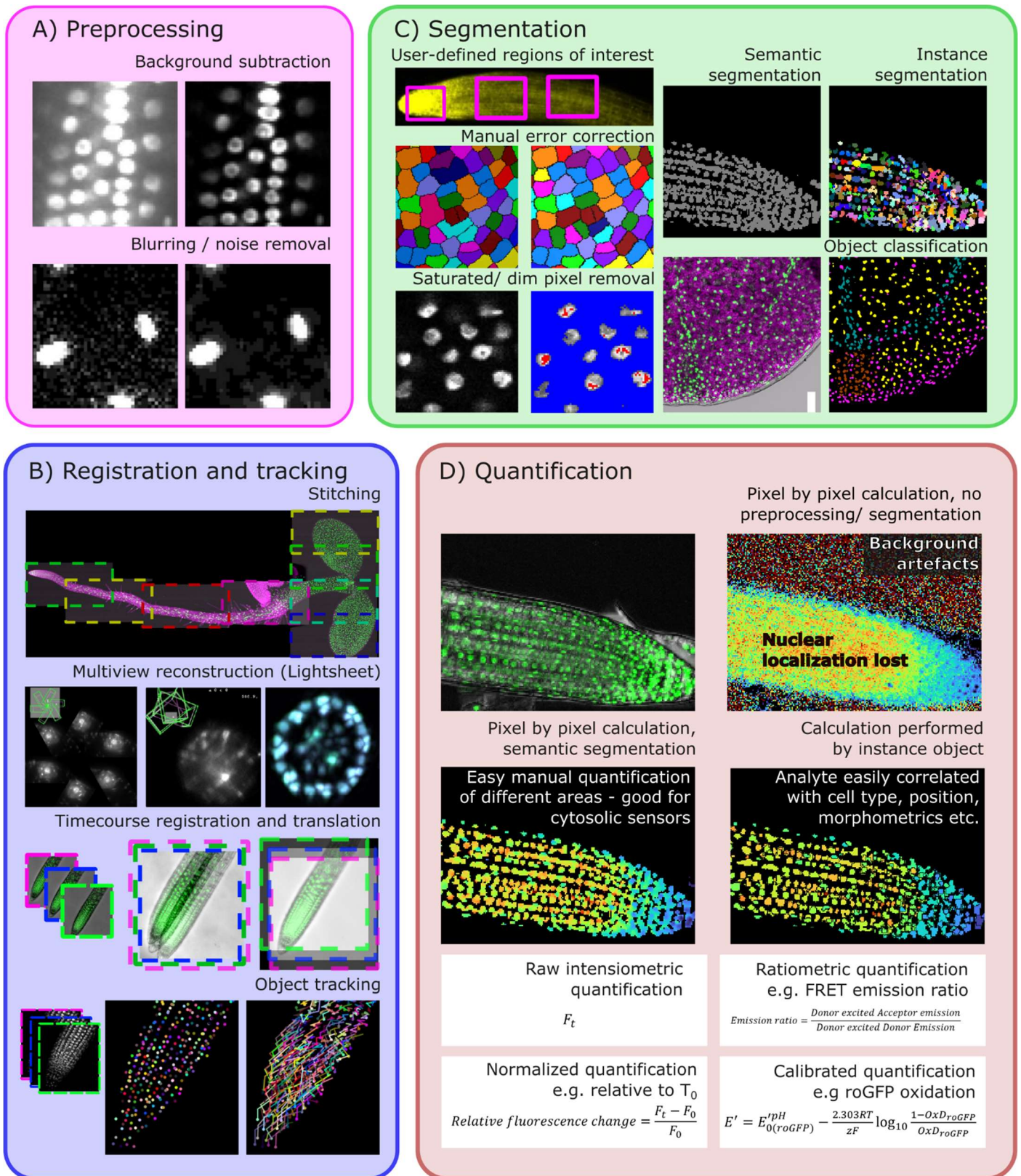
697
698
699
700
701
702
703
704
705
706
707
708
709
710
711
712
713
714
715
716

Figure 2. The many paths of biosensor deployment . Successful integration of engineered sensors into diverse biological systems requires meticulous design and testing across multiple stages. *In vitro*, purified sensors function as reporters to detect and quantify ligands. In heterologous systems like *E. coli*, yeast cells, and protoplasts, these sensors serve as effective screening tools, facilitating transporter identification among other applications. The *N. benthamiana* transient system is a standard preliminary platform for *in planta* sensor validation prior to the generation of stable transgenic lines. Codon optimization tailored to the target species along with the testing of suitable promoters and terminators is required to ensure robust expression and mitigate silencing. Utilization of various signaling peptides allows for sensor targeting to distinct subcellular locations in both transient and stable plant systems. In all applications, biosensor response is examined for dynamic range of response in artificially low and high analyte conditions to confirm sensor compatibility for detecting endogenous dynamics with sufficient SNR. In stable transgenic plants, sensor interaction with endogenous components can be revealed either by artefacts detected with low-affinity or non-responsive (NR) control sensors or by host plant phenotypes caused by sensor overexpression. Such evidence of non-orthogonality can necessitate re-engineering to reduce or remove interference with native signaling pathways. Once expressed in the target subcellular locale within the cells of the organism of interest and having been tested for orthogonality and response in the physiological range of the sensing target, direct biosensors are often highly transferrable parts ready for investigation in a range of organs and conditions as well as stable genetic introduction into further model plants or crops systems when combined with suitable expression cassettes and delivery vectors.



717
718 **Figure 3. Biosensor imaging.** Laser scanning Confocal microscopy (LSCM) is the most widely used method
719 as it offers versatility in terms of spatial resolution (from the use of different magnifications and tunable
720 resolution and super-resolution modalities for cell biology e.g. Airy Scan), temporal resolution (methods
721 such as resonant scanning and spinning disk microscopy can increase imaging speed), and allows
722 multichannel imaging. LSCM used for static end-point imaging offers high spatial resolution, but destructive
723 mounting limits temporal resolution and environmental control (Figure 3A). Buffer exchange setups are an
724 alternative to track the same sample before and after treatment and are a standard approach for *in planta*
725 validation of biosensors function (Figure 3C). Quantitative imaging often requires using a live imaging set-
726 up allowing the plant/or tissue to grow in controlled light, growing medium, temperature, and orientation,

727 to reflect a native environment. The use of microfluidic devices has been popularized in recent years to
728 combine high spatial resolution (LSCM) with time-course imaging, root tracking (see Box 4), and easily
729 tuned treatments (Figure 3D) (3, 67, 97). However, microfluidic devices are technically difficult to set up,
730 with most existing designs focusing on Arabidopsis roots. Cover-glass chambers are an easy to set
731 alternative for time-course imaging of seedlings offering controlled conditions (e.g. gravitropic response in
732 root and shoot (Figure 3E), or ABA dynamics in response to humidity stress using Nunc Lab-Tek chambers
733 (Rowe 2023)). New designs of imaging devices to perform controlled-condition live-imaging of other tissues
734 (leaves, shoot apical meristem, etc.) and plant models are essential. Despite its versatility, 3D imaging of
735 samples with LSCM is a slow process and extended period of high laser power can photobleach
736 fluorophores and damage tissues. Light Sheet Fluorescence Microscopy (LSFM) permits four-dimensional
737 imaging (High spatial and temporal dynamics) of an entire cell or tissue (Figure 3F) (132, 143) with low laser
738 intensity. Despite live-imaging of developing Arabidopsis seedlings or dissected tissues being feasible, FEP
739 tubes used in LSFM setups cannot accommodate large samples without major technical adjustments. Also,
740 LSFM large complex imaging outputs require challenging processing and analysis (see Box 4). Biosensors
741 imaging in deep tissues can also be achieved using embedded samples (45), or with fixed samples using the
742 clearsee method (61, 156), but those these are destructive and sacrifice temporal resolution. Among the
743 other common imaging techniques for biosensors, stereomicroscopy, epifluorescence and macro-imaging
744 allow non-destructive imaging of large samples and have been used to monitor rapid and “long-term” Ca^{2+}
745 or glutamate dynamics in Arabidopsis shoots (Figure 3G) (14, 64, 152). Stereomicroscopy or
746 spectrophotometry can alternatively be used as a “high throughput” biosensors imaging approach by using
747 96 well plates (Figure 3H). This approach also conditionally offers high spatial resolution if applied with
748 subcellular-targeted sensors (e.g. RoGFPs targeted to the chloroplasts, cytosol, or mitochondria (153)).
749
750



751
752
753
754
755
756
757
758
759
760
761
762

Figure 4. Four key steps that make up a typical image analysis pipeline. A Preprocessing involves image adjustments that will ease downstream analysis/segmentation steps, such as background subtraction or noise removal. **B** Registration and tracking involves finding the same objects or features between images. This allows multi stage-position images to be stitched, and Light Sheet multiview acquisitions to be merged. For timecourses, translation can remove object movement artefacts, and tracking post segmentation can allow powerful downstream analysis. **C** Segmentation divides the image into different areas to be analyzed separately, either with user drow boxes, or with algorithmic methods. There are different approaches depending on the use case e.g. Semantic segmentation (just sensor vs not sensor), instance segmentation (each object is labelled separately), object classification (classifying each instance of an object, e.g. cell types). Dim/saturated pixels may be removed at this stage, and segmentation errors manually corrected. **D** Quantification outputs will depend on upstream processing. Calculation can be performed on a pixel by

763
764
765

pixel basis, or object by object. Different sensor types will require different analysis methods, but normalized/ratiometric analysis is preferred to unaltered intensimetric outputs.

766

Table 1 Current generation genetically encoded fluorescent biosensors in plants

Biosensor Name	Target Analyte	<i>In vivo</i> SNR	Notable Applications/Findings	Usage citation
nlsABACUS2	ABA	**	Investigated ABA accumulation under abiotic stress and stomatal defense against spider mite infestation.	(131, 132)
ABALEONSD1-3L21	ABA	*	Multiplexed with Ca ²⁺ and H ⁺ sensors to demonstrate that ABA does not trigger fast cytosolic calcium or pH changes in roots, unlike stomata.	(159)
SNACS	ABA signalling (SnRK2 activity)	*	Showed CO ₂ and MeJA do not activate ABA signalling, but require basal signalling levels to elicit stomatal closure.	(170)
Amtrac1	Ammonium import	**	Demonstrated ammonium transporter activity.	(38)
ATeam AT1.03-nD/nA	ATP (MgATP ²⁻)	**	Visualized ATP balancing between compartments in Arabidopsis; showed differences in ATP levels between chloroplasts and cytosol under various conditions.	(37, 101)
AuxSen	Auxin	**	Used to measure auxin dynamics in roots and shoots.	(70)
DR5v2	Auxin	**	Indirect analysis of auxin used to investigate auxin related development.	(99)
DII-VENUS	Auxin	*	Indirect analysis of auxin	(19)
GCaMP6s	Ca ²⁺	****	Glutamate induction of calcium and electrical signaling from roots to shoots	(139)
R-GECO1	Ca ²⁺	***	Used for high-resolution imaging of calcium dynamics in response to environmental stimuli.	(72, 159)
NRCG-GECO1	Ca ²⁺	***	Demonstrated nuclear Ca ²⁺ spiking preceding cytosolic oscillation in <i>Medicago truncatula</i> .	(83, 96)
R-GECO1-mTurquoise	Ca ²⁺	***	Demonstrated ABA-induced Ca ²⁺ transients enhancing stomatal closure.	(160)
YC3.6	Ca ²⁺	**	Revealed the spatial and temporal dynamics of Ca ²⁺ during pollen tube growth	(57)
GPS2	GA	**	Showed GA accumulation during nodule development; helped understand GA's role in root and nodule growth.	(45, 66)
iGluSnFR	Glutamate	****	Investigated glutamate signaling in response to osmotic stress and wounding.	(25)
HyPer7	H ₂ O ₂	**	Applied to quantify flg22 ROS responses with high specificity.	(154)
cpFLIPPi	Inorganic phosphate	**	Showed different phosphate levels between organs and organelles in plants; demonstrated Pi flux in AMF-colonized cells.	(68, 118)
Jas9-Venus	JA-Ile	*	Indirect analysis of jasmonic acid during herbivore attack.	(92)
SoNaR	NADH/NAD ⁺	**	Elucidated NADH dynamics during pollen tube elongation and stomatal opening.	(101, 104)
iNAP	NADPH	**	Demonstrated export of reducing equivalents from chloroplasts supporting photorespiration in mitochondria.	(103)
NitraMeter3.0	Nitrate	**	Detected distinct nitrate levels in different root cells; analyzed local nitrate accumulation dynamics.	(29)
Nitrac	Nitrate import	*	Replicated dual affinity uptake kinetics of the CHL1/NRT1.1 protein.	(71)
PR1	Salicylic acid	**	Indirect analysis of salicylic acid during pathogen attack.	(22)
FLIPsuc	Sucrose	**	Used to discover SWEET family transporters	(28, 89)
SweetTrac1	Sucrose transport	**	Sucrose transporter (SWEET1) based sensor used to decode transport kinetics and function.	(123)
mCitrine-PH ^{PLC}	PI(4,5)P ₂	**	Used to study PI(4,5)P ₂ accumulation patterns across the shoot apical meristem.	(147)
cYFP-2xPH ^{PLC}	PI(4,5)P ₂	**	Investigated PI(4,5)P ₂ dynamics in plant cells, particularly in root hair elongation and organ initiation.	(146)

mCitrine-P4M ^{SidM}	PI(4)P	**	Investigated PI(4)P patterns across the shoot apical meristem.	(147)
2xCherry-PH ^{FAPP1}	PI(4)P	**	Investigated PI(4)P dynamics in plant cells, particularly in root hair elongation and organ initiation.	(142)
FP-N160 ^{RbohD}	Phosphatidic acid (PA)	**	Used to monitor PA dynamics in root apex upon gravistimulation	(73)
apo-pHusion	Apoplastic pH		Used to measure pH in the apoplastic acidification after auxin application	(55)
Acidin2/3/4	pH	**	Used to measure low pH on the apo- and cytoplasmic PM sides in root	(116)
pHcyto-PM	pH	**	Used to measure pH on the cytosolic side of the PM	(97, 107)

767

768 Summary Points

769 Genetically-encoded fluorescent biosensors have emerged as crucial tools for quantifying energetic,
770 metabolic, signaling molecules, and second messengers in plants, providing real-time data across various
771 scales from subcellular dynamics to whole-plant patterns.

- 772 • **Advancements in Energetics:** The use of ATP and NADH/NAD⁺ sensors like ATeam AT1.03-nD/nA
773 and SoNaR has revealed the intricate dynamics of ATP: NADPH balance, demonstrating significant
774 differences in energy distribution within cellular compartments under varying environmental
775 conditions.
- 776 • **Metabolic Discoveries:** Biosensors such as FLIPsuc for sucrose and iNAP for NADPH have elucidated
777 the complex processes of sugar transport and metabolic flux, offering insights into plant energy
778 management and inter-organ communication.
- 779 • **Signaling Pathway Insights:** Calcium biosensors like R-GECO1, GCaMPs and YC3.6 have uncovered
780 the temporal and spatial intricacies of Ca²⁺ signaling, particularly in stomatal regulation and stress
781 responses, highlighting the importance of calcium dynamics in plant physiology.
- 782 • **Hormonal Regulation:** The deployment of biosensors such as ABALEON and nlsABACUS2 for
783 abscisic acid (ABA) and GPS2 for gibberellins (GA) has facilitated the study of hormone distribution
784 and signaling, revealing their roles in development and stress adaptation.
- 785 • **ROS Monitoring:** Oxidation sensors like roGFP2-Orp1 and HyPer7 have enabled precise tracking of
786 reactive oxygen species (ROS) in response to environmental stress, offering new perspectives on
787 the oxidative burst and its regulatory mechanisms in plant immunity.
- 788 • **Nutrient Dynamics:** The cpFLIPPi sensor revealed inorganic phosphate levels and dynamics within
789 different cellular compartments, shedding light on phosphate's role in photosynthesis and nutrient
790 allocation, and Nitrameter has been used to visualize nitrate levels.
- 791 • **Technological Innovations:** Advancements in biosensor engineering, including the development of
792 high-throughput screening methods and AI-driven design are accelerating the creation of new
793 sensors with enhanced specificity and dynamic range.
- 794 • **Future Directions:** The integration of biosensor data with emerging 'omics' technologies and
795 advanced imaging techniques holds promise for a more comprehensive understanding of plant
796 systems biology, enabling detailed modeling and prediction of plant responses to various stimuli.

797 Terms and Definitions

- 798 • **Intensiometric** - Sensor output is a single emission intensity, which correlates with concentration of
799 the analyte or amount of a biological process.
- 800 • **Ratiometric** - Sensor output is a ratio of two different emission intensities, which controls for many
801 optical artefacts.
- 802 • **Orthogonal** – A fully orthogonal sensor does not interfere with endogenous machinery and
803 endogenous machinery does not interfere with sensor function.
- 804 • **Segmentation** – Using image analysis methods to determine which parts of an image to analyze.

- 805 • Dynamic range of response – The range of fluorescence change (output) of the sensor.
- 806 • Dynamic range of detection – The range of analyte concentrations that the sensor can detect.
- 807 • Signal-to-noise ratio (SNR) – The dynamic range of response relative to the noise inherent in
- 808 biological imaging.
- 809 • FRET (Forster Resonance Energy Transfer) – Energy transfer between a pair of fluorophores with
- 810 overlapping emission/excitation status that occurs at close proximity and at certain orientations.
- 811 • Multiplexing/multisensing – coexpression of multiple sensors for simultaneous quantification of
- 812 multiple analytes.
- 813 • Microfluidics – Small custom designed imaging chambers which allow fine control of environmental
- 814 conditions allowing fast treatment changes through buffer exchanges and high spatiotemporal
- 815 imaging.
- 816 • Spectral overlap – overlapping excitation or emission spectra, which can create a problem for
- 817 multiplexing sensors, or imaging sensors with dyes/other markers.

818 References annotations (up to 10, 20 words each)

- 819 • Biosensor reengineering for increased affinity, orthogonality and signal-to-noise and advanced
- 820 imaging and analysis used to explain a novel abiotic stress response
 - 821 ○ Rowe J, Grangé-Guermente M, Exposito-Rodriguez M, Wimalasekera R, Lenz MO, et al. 2023.
 - 822 Next-generation ABACUS biosensors reveal cellular ABA dynamics driving root growth at low
 - 823 aerial humidity. *Nature Plants* 2023, pp. 1–13
- 824 • Reengineering of a hormone biosensor to increase orthogonality and reversibility, used to unpick
- 825 the role of GA in apical hook development and opening
 - 826 ○ Griffiths J, Rizza A, Tang B, Frommer WB, Jones AM. 2023. Gibberellin Perception Sensors 1
 - 827 and 2 reveal cellular GA dynamics articulated by COP1 and GA20ox1 that are necessary but
 - 828 not sufficient to pattern hypocotyl cell elongation. bioRxiv. 2023.11.06.565859
- 829 • Deployment a phosphate biosensor into *Brachypodium*, to track how the flow of nutrients varies
- 830 with arbuscules
 - 831 ○ Zhang S, Daniels DA, Ivanov S, Jurgensen L, Müller LM, et al. 2022. A genetically encoded
 - 832 biosensor reveals spatiotemporal variation in cellular phosphate content in *Brachypodium*
 - 833 *distachyon* mycorrhizal roots. *New Phytologist*. 234(5):1817–31
- 834 • Multiplexed sensors used to dissect ABA and calcium responses at exquisite spatiotemporal
- 835 resolution
 - 836 ○ Waadt R, Krebs M, Kudla J, Schumacher K. 2017. Multiparameter imaging of calcium and
 - 837 abscisic acid and high-resolution quantitative calcium measurements using R-GECO1-
 - 838 mTurquoise in *Arabidopsis*. *New Phytologist*. 216(1):303–20
- 839 • Elegant demonstration of how the flow of reductants between organelles balances energetics *in*
- 840 *planta*, only achievable through biosensors
 - 841 ○ Voon CP, Guan X, Sun Y, Sahu A, Chan MN, et al. 2018. ATP compartmentation in plastids and
 - 842 cytosol of *Arabidopsis thaliana* revealed by fluorescent protein sensing. *Proc Natl Acad Sci U*
 - 843 *S A*. 115(45):E10778–87
- 844 • Comprehensive work demonstrating high throughput biosensor imaging to disentangle
- 845 mitochondrial retrograde signaling
 - 846 ○ Kasim Khan A, Cuong Tran H, Mansuroglu B, Costa A, Rasmusson AG, et al. 2024.
 - 847 Mitochondria-derived reactive oxygen species are the likely primary trigger of mitochondrial
 - 848 retrograde signaling in *Arabidopsis*. *Current Biology*. 34:327-342.e4
- 849 • Use of nlsABACUS2 and indirect auxin and plasmodesmata indicators to show how hormone fluxes
- 850 in primary roots growing across air gaps inhibit lateral root formation
 - 851 ○ Mehra P, Pandey BK, Melebari D, Banda J, Leftley N, et al. 2022. Hydraulic flux-responsive
 - 852 hormone redistribution determines root branching. *Science* (1979). 378(6621):762–68

- 853 • Macro R-GECO1 and iGluSnFR imaging demonstrating systemic L-Glutamate release under osmotic
854 stress and wounding required for the AtGLR3.3 mediated calcium wave
 - 855 ○ Grenzi M, Buratti S, Parmagnani AS, Abdel Aziz I, Bernacka-Wojcik I, et al. 2023. Long-
856 distance turgor pressure changes induce local activation of plant glutamate receptor-like
857 channels. *Current Biology*. 33(6):1019-1035.e8
- 858 • Unpicking biochemical limitations and transport in different root tissues using cell-type specific
859 perturbations, parameterizing a predictive model of hormone homeostasis
- 860 • Efficient engineering methods to develop a ratiometric sensor from an intensimetric sensor.
 - 861 ○ Ejike JO, Sadoine M, Shen Y, Ishikawa Y, Sunal E, et al. 2024. A Monochromatically Excitable
862 Green-Red Dual-Fluorophore Fusion Incorporating a New Large Stokes Shift Fluorescent
863 Protein. *Biochemistry*. 63(1):171–80
- 864 • Excellent high throughput repurposing of a ligand-dependent protein interaction pair, changing
865 specificity to accept diverse analytes
 - 866 ○ Beltrán J, Steiner PJ, Bedewitz M, Wei S, Peterson FC, et al. 2022. Rapid biosensor
867 development using plant hormone receptors as reprogrammable scaffolds. *Nature*
868 *Biotechnology* 2022 40:12. 40(12):1855–61

869 References cited

- 870 1. Abramson J, Adler J, Dunger J, Evans R, Green T, et al. 2024. Accurate structure prediction of
871 biomolecular interactions with AlphaFold 3. *Nature*
- 872 2. Akerboom J, Chen TW, Wardill TJ, Tian L, Marvin JS, et al. 2012. Optimization of a GCaMP
873 calcium indicator for neural activity imaging. *Journal of Neuroscience*. 32(40):13819–40
- 874 3. Allan C, Tayagui A, Hornung R, Nock V, Meisrimler CN. 2023. A dual-flow RootChip enables
875 quantification of bi-directional calcium signaling in primary roots. *Front Plant Sci*. 13:1040117
- 876 4. Allen GJ, Chu SP, Harrington CL, Schumacher K, Hoffmann T, et al. 2001. A defined range of
877 guard cell calcium oscillation parameters encodes stomatal movements. *Nature* 2001
878 411:6841. 411(6841):1053–57
- 879 5. Allen GJ, Kwak JM, Chu SP, Llopis J, Tsien RY, et al. 1999. Cameleon calcium indicator reports
880 cytoplasmic calcium dynamics in Arabidopsis guard cells. *The Plant Journal*. 19(6):735–47
- 881 6. Allen GJ, Kwak JM, Chu SP, Llopis J, Tsien RY, et al. 1999. Cameleon calcium indicator reports
882 cytoplasmic calcium dynamics in Arabidopsis guard cells. *Plant Journal*. 19(6):735–47
- 883 7. Andres J, Schmunk LJ, Grau-Enguix F, Braguy J, Samodelov SL, et al. 2024. Ratiometric
884 gibberellin biosensors for the analysis of signaling dynamics and metabolism in plant
885 protoplasts. *The Plant Journal*. 118(4):927–39
- 886 8. Aratani Y, Uemura T, Hagihara T, Matsui K, Toyota M. 2023. Green leaf volatile sensory calcium
887 transduction in Arabidopsis. *Nature Communications* 2023 14:1. 14(1):1–16
- 888 9. Ast C, Foret J, Oltrogge LM, De Michele R, Kleist TJ, et al. 2017. Ratiometric Matryoshka
889 biosensors from a nested cassette of green- and orange-emitting fluorescent proteins. *Nature*
890 *Communications* 2017 8:1. 8(1):1–13
- 891 10. Ast C, Foret J, Oltrogge LM, De Michele R, Kleist TJ, et al. 2017. Ratiometric Matryoshka
892 biosensors from a nested cassette of green- and orange-emitting fluorescent proteins. *Nat*
893 *Commun*. 8(1):
- 894 11. Balcerowicz M, Shetty KN, Jones AM. 2021. O auxin, where art thou? *Nature Plants* 2021 7:5.
895 7(5):546–47
- 896 12. Balcerowicz M, Shetty KN, Jones AM. 2021. Fluorescent biosensors illuminating plant
897 hormone research. *Plant Physiol*. 187(2):590–602
- 898 13. Barbez E, Dünser K, Gaidora A, Lendl T, Busch W. 2017. Auxin steers root cell expansion via
899 apoplastic pH regulation in Arabidopsis thaliana. *Proc Natl Acad Sci U S A*. 114(24):E4884–93
- 900 14. Bellandi A, Papp D, Breakspear A, Joyce J, Johnston MG, et al. 2022. Diffusion and bulk flow of
901 amino acids mediate calcium waves in plants. *Sci Adv*. 8(42):6693
- 902

- 903 15. Belousov V V., Fradkov AF, Lukyanov KA, Staroverov DB, Shakhbazov KS, et al. 2006.
904 Genetically encoded fluorescent indicator for intracellular hydrogen peroxide. *Nat Methods*.
905 3(4):281–86
- 906 16. Beltrán J, Steiner PJ, Bedewitz M, Wei S, Peterson FC, et al. 2022. Rapid biosensor
907 development using plant hormone receptors as reprogrammable scaffolds. *Nature*
908 *Biotechnology* 2022 40:12. 40(12):1855–61
- 909 17. Binci F, Offer E, Crosino A, Sciascia I, Kleine-Vehn J, et al. 2024. Spatially and temporally
910 distinct Ca²⁺ changes in Lotus japonicus roots orient fungal-triggered signalling pathways
911 towards symbiosis or immunity. *J Exp Bot*. 75(2):605–19
- 912 18. Brost C, Studtrucker T, Reimann R, Denninger P, Czekalla J, et al. 2019. Multiple cyclic
913 nucleotide-gated channels coordinate calcium oscillations and polar growth of root hairs.
914 *Wiley Online Library* C Brost, T Studtrucker, R Reimann, P Denninger, J Czekalla, M Krebs, B
915 *Fabry* *The Plant Journal*, 2019 • *Wiley Online Library*. 99(5):910–23
- 916 19. Brunoud G, Wells DM, Oliva M, Larrieu A, Mirabet V, et al. 2012. A novel sensor to map auxin
917 response and distribution at high spatio-temporal resolution
- 918 20. Brunoud G, Wells DM, Oliva M, Larrieu A, Mirabet V, et al. 2012. A novel sensor to map auxin
919 response and distribution at high spatio-temporal resolution
- 920 21. Bryant P, Pozzati G, Elofsson A. 2022. Improved prediction of protein-protein interactions using
921 AlphaFold2. *Nature Communications* 2022 13:1. 13(1):1–11
- 922 22. Caillaud MC, Asai S, Rallapalli G, Piquerez S, Fabro G, Jones JDG. 2013. A Downy Mildew
923 Effector Attenuates Salicylic Acid–Triggered Immunity in Arabidopsis by Interacting with the
924 Host Mediator Complex. *PLoS Biol*. 11(12):614–20099
- 925 23. Cao L, Coventry B, Goreshnik I, Huang B, Sheffler W, et al. 2022. Design of protein-binding
926 proteins from the target structure alone. *Nature* 2022 605:7910. 605(7910):551–60
- 927 24. Capoen W, Sun J, Wysham D, Otegui MS, Venkateshwaran M, et al. 2011. Nuclear membranes
928 control symbiotic calcium signaling of legumes. *Proc Natl Acad Sci U S A*. 108(34):14348–53
- 929 25. Castro-Rodríguez V, Kleist TJ, Gappel NM, Atanjaoui F, Okumoto S, et al. 2022. Sponging of
930 glutamate at the outer plasma membrane surface reveals roles for glutamate in development.
931 *The Plant Journal*. 109(3):664–74
- 932 26. Chater C, Peng K, Movahedi M, Dunn JA, Walker HJ, et al. 2015. Elevated CO₂-Induced
933 Responses in Stomata Require ABA and ABA Signaling. *Current Biology*. 25(20):2709–16
- 934 27. Chen LQ, Hou BH, Lalonde S, Takanaga H, Hartung ML, et al. 2010. Sugar transporters for
935 intercellular exchange and nutrition of pathogens. *Nature*. 468(7323):527–32
- 936 28. Chen LQ, Qu XQ, Hou BH, Sosso D, Osorio S, et al. 2012. Sucrose efflux mediated by SWEET
937 proteins as a key step for phloem transport. *Science (1979)*. 335(6065):207–11
- 938 29. Chen YN, Cartwright HN, Ho CH. 2022. In vivo visualization of nitrate dynamics using a
939 genetically encoded fluorescent biosensor. *Sci Adv*. 8(42):4915
- 940 30. Chevalier A, Silva DA, Rocklin GJ, Hicks DR, Vergara R, et al. 2017. Massively parallel de novo
941 protein design for targeted therapeutics. *Nature* 2017 550:7674. 550(7674):74–79
- 942 31. Chiu C-L, Clack N, community the napari. 2022. napari: a Python Multi-Dimensional Image
943 Viewer Platform for the Research Community. *Microscopy and Microanalysis*. 28(S1):1576–77
- 944 32. Choi WG, Toyota M, Kim SH, Hilleary R, Gilroy S. 2014. Salt stress-induced Ca²⁺ waves are
945 associated with rapid, long-distance root-to-shoot signaling in plants. *Proc Natl Acad Sci U S A*.
946 111(17):6497–6502
- 947 33. Clark NM, Elmore JM, Walley JW. 2022. To the proteome and beyond: advances in single-cell
948 omics profiling for plant systems. *Plant Physiol*. 188(2):726–37
- 949 34. Cohen JD, Strader LC. 2024. An auxin research odyssey: 1989–2023. *Plant Cell*. 36(5):1410–28
- 950 35. Colin L, Martin-Arevalillo R, Bovio S, Bauer A, Vernoux T, et al. 2022. Imaging the living plant
951 cell: From probes to quantification. *Plant Cell*. 34(1):247–72
- 952 36. De Chaumont F, Dallongeville S, Chenouard N, Hervé N, Pop S, et al. 2012. Icy: An open
953 bioimage informatics platform for extended reproducible research

- 954 37. De Col V, Fuchs P, Nietzel T, Elsässer M, Voon CP, et al. 2017. ATP sensing in living plant cells
955 reveals tissue gradients and stress dynamics of energy physiology. *Elife*. 6:
- 956 38. De Michele R, Ast C, Loqué D, Ho CH, Andrade SLA, et al. 2013. Fluorescent sensors reporting
957 the activity of ammonium transporters in live cells. *Elife*. 2013(2):
- 958 39. de Reuille PB, Routier-Kierzkowska A-LL, Kierzkowski D, Bassel GW, Schüpbach T, et al. 2015.
959 MorphoGraphX: A platform for quantifying morphogenesis in 4D. *Elife*. 4(MAY):e05864
- 960 40. Decaestecker W, Buono RA, Pfeiffer ML, Vangheluwe N, Jourquin J, et al. 2019. CRISPR-TSKO: A
961 Technique for Efficient Mutagenesis in Specific Cell Types, Tissues, or Organs in Arabidopsis.
962 *Plant Cell*. 31(12):2868–87
- 963 41. Deuschle K, Chaudhuri B, Okumoto S, Lager I, Lalonde S, Frommer WB. 2006. Rapid
964 Metabolism of Glucose Detected with FRET Glucose Nanosensors in Epidermal Cells and Intact
965 Roots of Arabidopsis RNA-Silencing Mutants. *Plant Cell*. 18(9):2314–25
- 966 42. Deuschle K, Chaudhuri B, Okumoto S, Lager I, Lalonde S, Frommer WB. 2006. Rapid
967 metabolism of glucose detected with FRET glucose nanosensors in epidermal cells and intact
968 roots of Arabidopsis RNA-silencing mutants. *Plant Cell*. 18(9):2314–25
- 969 43. Dindas J, Scherzer S, Roelfsema MRG, Von Meyer K, Müller HM, et al. 2018. AUX1-mediated
970 root hair auxin influx governs SCFTIR1/AFB-type Ca²⁺ signaling. *Nature Communications* 2018
971 9:1. 9(1):1–10
- 972 44. Doumane M, Lebecq A, Colin L, Fangain A, Stevens FD, et al. 2021. Inducible depletion of
973 PI(4,5)P₂ by the synthetic iDePP system in Arabidopsis. *Nature Plants* 2021 7:5. 7(5):587–97
- 974 45. Drapek C, Rizza A, Mohd-Radzman NA, Schiessl K, Dos Santos Barbosa F, et al. 2024.
975 Gibberellin dynamics governing nodulation revealed using GIBBERELLIN PERCEPTION SENSOR
976 2 in *Medicago truncatula* lateral organs. *Plant Cell*
- 977 46. Duan L, Dietrich D, Ng CH, Yeen Chan PM, Bhalerao R, et al. 2013. Endodermal ABA signaling
978 promotes lateral root quiescence during salt stress in Arabidopsis seedlings. *Plant Cell*.
979 25(1):324–41
- 980 47. Ejike JO, Sadoine M, Shen Y, Ishikawa Y, Sunal E, et al. 2024. A Monochromatically Excitable
981 Green-Red Dual-Fluorophore Fusion Incorporating a New Large Stokes Shift Fluorescent
982 Protein. *Biochemistry*. 63(1):171–80
- 983 48. Elsässer M, Feitosa-Araujo E, Lichtenauer S, Wagner S, Fuchs P, et al. 2020. Photosynthetic
984 activity triggers pH and NAD redox signatures across different plant cell compartments.
985 *bioRxiv*. 2020.10.31.363051
- 986 49. Engler C, Youles M, Gruetzner R, Ehnert TM, Werner S, et al. 2014. A Golden Gate modular
987 cloning toolbox for plants. *ACS Synth Biol*. 3(11):839–43
- 988 50. Evans MJ, Choi WG, Gilroy S, Morris RJ. 2016. A ROS-Assisted Calcium Wave Dependent on the
989 AtRBOHD NADPH Oxidase and TPC1 Cation Channel Propagates the Systemic Response to Salt
990 Stress. *Plant Physiol*. 171(3):1771–84
- 991 51. Exposito-Rodriguez M, Laissie PP, Yvon-Durocher G, Smirnoff N, Mullineaux PM. 2017.
992 Photosynthesis-dependent H₂O₂ transfer from chloroplasts to nuclei provides a high-light
993 signalling mechanism. *Nat Commun*. 8(1):1–11
- 994 52. Exposito-Rodriguez M, Reeder B, Brooke GN, Hough MA, Laissie PP, Mullineaux PM. 2024. A
995 novel glutathione peroxidase-based biosensor disentangles differential subcellular
996 accumulation of H₂O₂ and lipid hydroperoxides. *bioRxiv*. 2024.01.18.576236
- 997 53. Fehr M, Frommer WB, Lalonde S. 2002. Visualization of maltose uptake in living yeast cells by
998 fluorescent nanosensors. *Proc Natl Acad Sci U S A*. 99(15):9846–51
- 999 54. Fendrych M, Akhmanova M, Merrin J, Glanc M, Hagihara S, et al. 2018. Rapid and reversible
000 root growth inhibition by TIR1 auxin signalling. *Nature Plants* 2018 4:7. 4(7):453–59
- 001 55. Fendrych M, Leung J, Friml J. 2016. Tir1/AFB-Aux/IAA auxin perception mediates rapid cell
002 wall acidification and growth of Arabidopsis hypocotyls. *Elife*. 5(September2016):
- 003 56. Fuchs R, Kopischke M, Klapprodt C, Hause G, Meyer AJ, et al. 2016. Immobilized
004 Subpopulations of Leaf Epidermal Mitochondria Mediate PENETRATION2-Dependent
005 Pathogen Entry Control in Arabidopsis. *Plant Cell*. 28(1):130–45

- 006 57. Gao QF, Gu LL, Wang HQ, Fei CF, Fang X, et al. 2016. Cyclic nucleotide-gated channel 18 is an
007 essential Ca²⁺ channel in pollen tube tips for pollen tube guidance to ovules in Arabidopsis.
008 *Proc Natl Acad Sci U S A.* 113(11):3096–3101
- 009 58. Gao YQ, Jimenez-Sandoval P, Tiwari S, Stolz S, Wang J, et al. 2023. Ricca's factors as mobile
010 proteinaceous effectors of electrical signaling. *Cell.* 186(7):1337-1351.e20
- 011 59. García-Calvo J, López-Andarias J, Maillard J, Mercier V, Roffay C, et al. 2022. HydroFlipper
012 membrane tension probes: imaging membrane hydration and mechanical compression
013 simultaneously in living cells. *Chem Sci.* 13(7):2086–93
- 014 60. Geiger D, Maierhofer T, Al-Rasheid KAS, Scherzer S, Mumm P, et al. 2011. Stomatal closure by
015 fast abscisic acid signaling is mediated by the guard cell anion channel SLAH3 and the receptor
016 RCAR1. *Sci Signal.* 4(173):
- 017 61. Gelderen K van van, Velde K van der, Kang C-K, Hollander J, Petropoulos O, et al. 2023.
018 Gibberellin transport affects (lateral) root growth through HY5 during Far-Red light
019 enrichment. *bioRxiv.* 2023.04.21.537844
- 020 62. Gjetting KSK, Ytting CK, Schulz A, Fuglsang AT. 2012. Live imaging of intra- and extracellular pH
021 in plants using pHusion, a novel genetically encoded biosensor. *J Exp Bot.* 63(8):3207–18
- 022 63. Greenwald EC, Mehta S, Zhang J. 2018. Genetically Encoded Fluorescent Biosensors Illuminate
023 the Spatiotemporal Regulation of Signaling Networks. *Chem Rev.* 118(24):11707–94
- 024 64. Grenzi M, Buratti S, Parmagnani AS, Abdel Aziz I, Bernacka-Wojcik I, et al. 2023. Long-distance
025 turgor pressure changes induce local activation of plant glutamate receptor-like channels.
026 *Current Biology.* 33(6):1019-1035.e8
- 027 65. Grenzi M, Resentini F, Vanneste S, Zottini M, Bassi A, Costa A. 2021. Illuminating the hidden
028 world of calcium ions in plants with a universe of indicators. *Plant Physiol.* 187(2):550–71
- 029 66. Griffiths J, Rizza A, Tang B, Frommer WB, Jones AM. 2024. GIBBERELLIN PERCEPTION SENSOR
030 2 reveals genesis and role of cellular GA dynamics in light-regulated hypocotyl growth. *Plant*
031 *Cell*
- 032 67. Grossmann G, Guo WJ, Ehrhardt DW, Frommer WB, Sit R V., et al. 2011. The RootChip: an
033 integrated microfluidic chip for plant science. *Plant Cell.* 23(12):4234–40
- 034 68. Gu H, Lalonde S, Okumoto S, Looger LL, Scharff-Poulsen AM, et al. 2006. A novel analytical
035 method for in vivo phosphate tracking. *FEBS Lett.* 580(25):5885–93
- 036 69. Hager A, Debus G, Edel HG, Stransky H, Serrano R. 1991. Auxin induces exocytosis and the
037 rapid synthesis of a high-turnover pool of plasma-membrane H(+)-ATPase. *Planta.* 185(4):527–
038 37
- 039 70. Herud-Sikimić O, Stiel AC, Kolb M, Shanmugaratnam S, Berendzen KW, et al. 2021. A biosensor
040 for the direct visualization of auxin. *Nature.* 592(7856):768–72
- 041 71. Ho CH, Frommer WB. 2014. Fluorescent sensors for activity and regulation of the nitrate
042 transceptor CHL1/NRT1.1 and oligopeptide transporters. *Elife.* 2014(3):
- 043 72. Huang S, Waadt R, Nuhkat M, Kollist H, Hedrich R, Roelfsema MRG. 2019. Calcium signals in
044 guard cells enhance the efficiency by which abscisic acid triggers stomatal closure. *New*
045 *Phytologist.* 224(1):177–87
- 046 73. Ito T, Wellmer F, Yu H, Das P, Ito N, et al. 2004. The homeotic protein AGAMOUS controls
047 microsporogenesis by regulation of SPOROCTELESS. *Nature.* 430(6997):356–60
- 048 74. Ito Y, Esnay N, Platre MP, Watted-Boyer V, Noack LC, et al. 2021. Sphingolipids mediate polar
049 sorting of PIN2 through phosphoinositide consumption at the trans-Golgi network. *Nature*
050 *Communications 2021 12:1.* 12(1):1–18
- 051 75. Jain P, Liu W, Zhu S, Chang CYY, Melkonian J, et al. 2021. A minimally disruptive method for
052 measuring water potential in planta using hydrogel nanoreporters. *Proc Natl Acad Sci U S A.*
053 118(23):e2008276118
- 054 76. Jedličková V, Naghani SE, Robert HS. 2022. On the trail of auxin: Reporters and sensors. *Plant*
055 *Cell.* 34(9):3200–3213
- 056 77. Jones AM. 2016. A new look at stress: Abscisic acid patterns and dynamics at high-resolution.
057 *New Phytologist.* 210(1):38–44

- 058 78. Jones AM, Danielson JÅH, ManojKumar SN, Lanquar V, Grossmann G, Frommer WB. 2014.
059 Abscisic acid dynamics in roots detected with genetically encoded FRET sensors. *Elife*.
060 3:e01741
- 061 79. Jubany-Mari T, Alegre-Batlle L, Jiang K, Feldman LJ. 2010. Use of a redox-sensing GFP (c-
062 roGFP1) for real-time monitoring of cytosol redox status in Arabidopsis thaliana water-
063 stressed plants. *FEBS Lett*. 584(5):889–97
- 064 80. Jumper J, Evans R, Pritzel A, Green T, Figurnov M, et al. 2021. Highly accurate protein structure
065 prediction with AlphaFold. *Nature*. 596(7873):583
- 066 81. Kaper T, Looger LL, Takanaga H, Platten M, Steinman L, Frommer WB. 2007. Nanosensor
067 Detection of an Immunoregulatory Tryptophan Influx/Kynurenine Efflux Cycle. *PLoS Biol*.
068 5(10):e257
- 069 82. Kasim Khan A, Cuong Tran H, Mansuroglu B, Costa A, Rasmusson AG, et al. 2024.
070 Mitochondria-derived reactive oxygen species are the likely primary trigger of mitochondrial
071 retrograde signaling in Arabidopsis. *Current Biology*. 34:327-342.e4
- 072 83. Kelner A, Leitão N, Chabaud M, Charpentier M, de Carvalho-Niebel F. 2018. Dual color sensors
073 for simultaneous analysis of calcium signal dynamics in the nuclear and cytoplasmic
074 compartments of plant cells. *Front Plant Sci*. 9:340652
- 075 84. Kleist TJ, Lin IW, Xu S, Maksaev G, Sadoine M, et al. 2022. OzTracs: Optical Osmolality
076 Reporters Engineered from Mechanosensitive Ion Channels. *Biomolecules*. 12(6):
- 077 85. Koveal D, Rosen PC, Meyer DJ, Díaz-García CM, Wang Y, et al. 2022. A high-throughput
078 multiparameter screen for accelerated development and optimization of soluble genetically
079 encoded fluorescent biosensors. *Nature Communications* 2022 13:1. 13(1):1–14
- 080 86. Kwak JM, Mori IC, Pei ZM, Leonhard N, Angel Torres M, et al. 2003. NADPH oxidase AtrbohD
081 and AtrbohF genes function in ROS-dependent ABA signaling in Arabidopsis. *EMBO J*.
082 22(11):2623–33
- 083 87. Kwak SY, Wong MH, Lew TTS, Bisker G, Lee MA, et al. 2017. Nanosensor technology applied to
084 living plant systems. *Annual Review of Analytical Chemistry*. 10(Volume 10, 2017):113–40
- 085 88. Lace B, Prandi C. 2016. Shaping Small Bioactive Molecules to Untangle Their Biological
086 Function: A Focus on Fluorescent Plant Hormones. *Mol Plant*. 9:1099–1118
- 087 89. Lager I, Looger LL, Hilpert M, Lalonde S, Frommer WB. 2006. Conversion of a putative
088 Agrobacterium sugar-binding protein into a FRET sensor with high selectivity for sucrose.
089 *Journal of Biological Chemistry*. 281(41):30875–83
- 090 90. Lambert TJ. 2019. FPbase: a community-editable fluorescent protein database. *Nat Methods*.
091 16(4):277–78
- 092 91. Lanquar V, Grossmann G, Vinkenborg JL, Merckx M, Thomine S, Frommer WB. 2014. Dynamic
093 imaging of cytosolic zinc in Arabidopsis roots combining FRET sensors and RootChip
094 technology. *New Phytologist*. 202(1):198–208
- 095 92. Larrieu A, Champion A, Legrand J, Lavenus J, Mast D, et al. 2015. A fluorescent hormone
096 biosensor reveals the dynamics of jasmonate signalling in plants. *Nature Communications*
097 2015 6:1. 6(1):1–9
- 098 93. Larsen B, Hofmann R, Camacho IS, Clarke RW, Clark Lagarias J, et al. 2023. Highlighter: An
099 optogenetic system for high-resolution gene expression control in plants. *PLoS Biol*.
100 21(9):e3002303
- 101 94. Laureyns R, Joossens J, Herwegh D, Pevernagie J, Pavie B, et al. 2022. An in situ sequencing
102 approach maps PLASTOCHRON1 at the boundary between indeterminate and determinate
103 cells. *Plant Physiol*. 188(2):782–94
- 104 95. Lee TA, Nobori T, Illouz-Eliaz N, Xu J, Jow B, et al. 2023. A Single-Nucleus Atlas of Seed-to-Seed
105 Development in Arabidopsis. *bioRxiv*. 2023.03.23.533992
- 106 96. Leitão N, Dangeville P, Carter R, Charpentier M. 2019. Nuclear calcium signatures are
107 associated with root development. *Nat Commun*. 10(1):

- 108 97. Li L, Verstraeten I, Roosjen M, Takahashi K, Rodriguez L, et al. 2021. Cell surface and
109 intracellular auxin signalling for H⁺ fluxes in root growth. *Nature* 2021 599:7884.
110 599(7884):273–77
- 111 98. Li T, Xiao X, Liu Q, Li W, Li L, et al. 2023. Dynamic responses of PA to environmental stimuli
112 imaged by a genetically encoded mobilizable fluorescent sensor. *Plant Commun.* 4(3):100500
- 113 99. Liao CY, Smet W, Brunoud G, Yoshida S, Vernoux T, Weijers D. 2015. Reporters for sensitive and
114 quantitative measurement of auxin response. *Nat Methods.* 12(3):207–10
- 115 100. Liese A, Eichstädt B, Lederer S, Schulz P, Oehlschläger J, et al. 2024. Imaging of plant calcium-
116 sensor kinase conformation monitors real time calcium-dependent decoding in planta. *Plant*
117 *Cell.* 36(2):276–97
- 118 101. Lim SL, Flütsch S, Liu J, Distefano L, Santelia D, Lim BL. 2022. Arabidopsis guard cell
119 chloroplasts import cytosolic ATP for starch turnover and stomatal opening. *Nature*
120 *Communications* 2022 13:1. 13(1):1–13
- 121 102. Lim S-L, Liu J, Dupouy G, Singh G, Baudrey S, et al. 2024. In planta imaging of pyridine
122 nucleotides using second-generation fluorescent protein biosensors. *The Plant Journal*
- 123 103. Lim S-L, Voon CP, Guan X, Yang Y, Gardeström P, Lim BL. 2020. In planta study of
124 photosynthesis and photorespiration using NADPH and NADH/NAD⁺ fluorescent protein
125 sensors. *Nat Commun.* 11(1):3238
- 126 104. Liu J, Lim SL, Zhong JY, Lim BL. 2022. Bioenergetics of pollen tube growth in Arabidopsis
127 thaliana revealed by ratiometric genetically encoded biosensors. *Nature Communications*
128 2022 13:1. 13(1):1–19
- 129 105. Liu L, Limsakul P, Meng X, Huang Y, Harrison RES, et al. 2021. Integration of FRET and
130 sequencing to engineer kinase biosensors from mammalian cell libraries. *Nature*
131 *Communications* 2021 12:1. 12(1):1–16
- 132 106. Liu Y, Yuan G, Hassan MM, Abraham PE, Mitchell JC, et al. 2022. Biological and Molecular
133 Components for Genetically Engineering Biosensors in Plants. *BioDesign Research.* 2022:
- 134 107. Martinière A, Gibrat R, Sentenac H, Dumont X, Gaillard I, Paris N. 2018. Uncovering pH at both
135 sides of the root plasma membrane interface using noninvasive imaging. *Proc Natl Acad Sci U*
136 *S A.* 115(25):6488–93
- 137 108. Maxwell K, Johnson GN. 2000. Chlorophyll fluorescence--a practical guide. *J Exp Bot.*
138 51(345):659–68
- 139 109. McAdam SAM, Brodribb TJ, Ross JJ. 2016. Shoot-derived abscisic acid promotes root growth.
140 *Plant Cell Environ.* 39(3):652–59
- 141 110. McMahan SM, Jackson MB. 2018. An Inconvenient Truth: Calcium Sensors Are Calcium Buffers
- 142 111. Mehra P, Pandey BK, Melebari D, Banda J, Leftley N, et al. 2022. Hydraulic flux–responsive
143 hormone redistribution determines root branching. *Science (1979).* 378(6621):762–68
- 144 112. Michels L, Gorelova V, Harnvanichvech Y, Borst JW, Albada B, et al. 2020. Complete
145 microviscosity maps of living plant cells and tissues with a toolbox of targeting
146 mechanoprobes. *Proc Natl Acad Sci U S A.* 117(30):18110–18
- 147 113. Miller G, Schlauch K, Tam R, Cortes D, Torres MA, et al. 2009. The plant NADPH oxidase
148 RBOHD mediates rapid systemic signaling in response to diverse stimuli. *Sci Signal.* 2(84):
- 149 114. Miyawaki A, Llopis J, Heim R, Mccaffery JM, Adams JA, et al. 1997. Fluorescent indicators for
150 Ca²⁺ based on green fluorescent proteins and calmodulin
- 151 115. Moe-Lange J, Gappel NM, Machado M, Wudick MM, Sies CSA, et al. 2021. Interdependence of
152 a mechanosensitive anion channel and glutamate receptors in distal wound signaling. *Sci Adv.*
153 7(37):
- 154 116. Moreau H, Gaillard I, Paris N. 2022. Genetically encoded fluorescent sensors adapted to acidic
155 pH highlight subdomains within the plant cell apoplast. *J Exp Bot.* 73(19):6744–57
- 156 117. Mousavi SAR, Chauvin A, Pascaud F, Kellenberger S, Farmer EE. 2013. GLUTAMATE RECEPTOR-
157 LIKE genes mediate leaf-to-leaf wound signalling. *Nature.* 500(7463):422–26

- 158 118. Mukherjee P, Banerjee S, Wheeler A, Ratliff LA, Irigoyen S, et al. 2015. Live Imaging of
159 Inorganic Phosphate in Plants with Cellular and Subcellular Resolution. *Plant Physiol.*
160 167(3):628–38
- 161 119. Nietzel T, Elsässer M, Ruberti C, Steinbeck J, Ugalde JM, et al. 2019. The fluorescent protein
162 sensor roGFP2-Orp1 monitors in vivo H₂O₂ and thiol redox integration and elucidates
163 intracellular H₂O₂ dynamics during elicitor-induced oxidative burst in Arabidopsis. *New*
164 *Phytologist.* 221(3):1649–64
- 165 120. Ochoa-Fernandez R, Abel NB, Wieland FG, Schlegel J, Koch LA, et al. 2020. Optogenetic control
166 of gene expression in plants in the presence of ambient white light. *Nature Methods* 2020
167 17:7. 17(7):717–25
- 168 121. Okumoto S, Jones A, Frommer WB. 2012. Quantitative imaging with fluorescent biosensors.
169 *Annu Rev Plant Biol.* 63(Volume 63, 2012):663–706
- 170 122. Østergaard H, Henriksen H, Henriksen A, Hansen FG, Winther JR. 2001. Shedding light on
171 disulfide bond formation: engineering a redox switch in green fluorescent protein. *EMBO J.*
172 20:5853–62
- 173 123. Park J, Chavez TM, Guistwhite JA, Gwon S, Frommer WB, Cheung LS. 2022. Development and
174 quantitative analysis of a biosensor based on the Arabidopsis SWEET1 sugar transporter. *Proc*
175 *Natl Acad Sci U S A.* 119(4):e2119183119
- 176 124. Platre MP, Noack LC, Doumane M, Bayle V, Simon MLA, et al. 2018. A Combinatorial Lipid
177 Code Shapes the Electrostatic Landscape of Plant Endomembranes. *Dev Cell.* 45(4):465-
178 480.e11
- 179 125. Postiglione AE, Muday GK. 2023. Abscisic acid increases hydrogen peroxide in mitochondria to
180 facilitate stomatal closure. *Plant Physiol.* 192(1):469–87
- 181 126. Qi L, Kwiatkowski M, Kulich I, Chen H, Gao Y, et al. 2023. Guanylate cyclase activity of TIR1/AFB
182 auxin receptors in rapid auxin responses. *bioRxiv.* 2023.11.18.567481
- 183 127. Raju AS, Kramer DM, Versaw WK. 2024. Genetically manipulated chloroplast stromal
184 phosphate levels alter photosynthetic efficiency. *Plant Physiol*
- 185 128. Riggs JW, Rockwell NC, Cavales PC, Callis J. 2016. Identification of the plant ribokinase and
186 discovery of a role for Arabidopsis Ribokinase in nucleoside metabolism. *Journal of Biological*
187 *Chemistry.* 291(43):22572–82
- 188 129. Rizza A, Tang B, Stanley CE, Grossmann G, Owen MR, et al. 2021. Differential biosynthesis and
189 cellular permeability explain longitudinal gibberellin gradients in growing roots. *Proceedings*
190 *of the National Academy of Sciences.* 118(8):e1921960118
- 191 130. Rizza A, Walia A, Lanquar V, Frommer WB, Jones AM. 2017. In vivo gibberellin gradients
192 visualized in rapidly elongating tissues. *Nat Plants.* 3(10):803–13
- 193 131. Rosa-Diaz I, Rowe J, Cayuela-Lopez A, Arbona V, Díaz I, Jones AM. 2024. Spider mite herbivory
194 induces an ABA-driven stomatal defense. *Plant Physiol*
- 195 132. Rowe J, Grangé-Guermente M, Exposito-Rodriguez M, Wimalasekera R, Lenz MO, et al. 2023.
196 Next-generation ABACUS biosensors reveal cellular ABA dynamics driving root growth at low
197 aerial humidity. *Nature Plants* 2023, pp. 1–13
- 198 133. Rusnak B, Clark FK, Vadde BVL, Roeder AHK. 2024. What Is a Plant Cell Type in the Age of
199 Single-Cell Biology? It’s Complicated. *Annu Rev Cell Dev Biol*
- 200 134. Sadoine M, Ishikawa Y, Kleist TJ, Wudick MM, Nakamura M, et al. 2021. Designs, applications,
201 and limitations of genetically encoded fluorescent sensors to explore plant biology. *Plant*
202 *Physiol.* 187(2):485–503
- 203 135. San Martín A, Ceballo S, Ruminot I, Lerchundi R, Frommer WB, Barros LF. 2013. A Genetically
204 Encoded FRET Lactate Sensor and Its Use To Detect the Warburg Effect in Single Cancer Cells.
205 *PLoS One.* 8(2):e57712
- 206 136. Scherschel M, Niemeier J-O, Jacobs LJHC, Hoffmann M, Diederich A, et al. 2024. The NAPstar
207 family of NADP redox state sensors highlights glutathione as the primary mediator of anti-
208 oxidative electron flux. *bioRxiv.* 2024.02.14.580349

- 209 137. Schindelin J, Arganda-Carreras I, Frise E, Kaynig V, Longair M, et al. 2012. Fiji: an open-source
210 platform for biological-image analysis. *Nat Methods*. 9(7):676
- 211 138. Shahan R, Hsu CW, Nolan TM, Cole BJ, Taylor IW, et al. 2022. A single-cell Arabidopsis root
212 atlas reveals developmental trajectories in wild-type and cell identity mutants. *Dev Cell*.
213 57(4):543-560.e9
- 214 139. Shao Q, Gao Q, Lhamo D, Zhang H, Luan S. 2020. Two glutamate- And pH-regulated
215 Ca²⁺channels are required for systemic wound signaling in Arabidopsis. *Sci Signal*. 13(640):
- 216 140. Shi B, Felipo-Benavent A, Cerutti G, Galvan-Ampudia C, Jilli L, et al. 2024. A quantitative
217 gibberellin signaling biosensor reveals a role for gibberellins in internode specification at the
218 shoot apical meristem. *Nature Communications* 2024 15:1. 15(1):1–18
- 219 141. Shih HW, Depew CL, Miller ND, Monshausen GB. 2015. The Cyclic Nucleotide-Gated Channel
220 CNGC14 Regulates Root Gravitropism in Arabidopsis thaliana. *Current Biology*. 25(23):3119–25
- 221 142. Shikata H, Sato Y, Schwechheimer C. 2023. Monitoring single root hairs using a micro-
222 chambered hydroponics system MiCHy reveals a new mode of action of the aminosteroid
223 U73122. *bioRxiv*. 2023.07.20.549431
- 224 143. Shkolnik D, Nuriel R, Bonza MC, Costa A, Fromm H. 2018. MIZ1 regulates ECA1 to generate a
225 slow, long-distance phloem-transmitted Ca²⁺ signal essential for root water tracking in
226 Arabidopsis. *Proc Natl Acad Sci U S A*. 115(31):8031–36
- 227 144. Siligato R, Wang X, Yadav SR, Lehesranta S, Ma G, et al. 2016. MultiSite Gateway-Compatible
228 Cell Type-Specific Gene-Inducible System for Plants. *Plant Physiol*. 170(2):627–41
- 229 145. Simon MLA, Platre MP, Assil S, Van Wijk R, Chen WY, et al. 2014. A multi-colour/multi-affinity
230 marker set to visualize phosphoinositide dynamics in Arabidopsis. *The Plant Journal*.
231 77(2):322–37
- 232 146. Simon MLA, Platre MP, Marquès-Bueno MM, Armengot L, Stanislas T, et al. 2016. A PtdIns(4)P-
233 driven electrostatic field controls cell membrane identity and signalling in plants. *Nature*
234 *Plants* 2016 2:7. 2(7):1–10
- 235 147. Stanislas T, Platre MP, Liu M, Rambaud-Lavigne LES, Jaillais Y, Hamant O. 2018. A
236 phosphoinositide map at the shoot apical meristem in Arabidopsis thaliana. *BMC Biol*.
237 16(1):1–13
- 238 148. Takanaga H, Chaudhuri B, Frommer WB. 2008. GLUT1 and GLUT9 as major contributors to
239 glucose influx in HepG2 cells identified by a high sensitivity intramolecular FRET glucose
240 sensor. *Biochim Biophys Acta Biomembr*. 1778(4):1091–99
- 241 149. Tan Y-Q, Yang Y, Zhang A, Fei C-F, Gu L-L, et al. 2020. Three CNGC family members, CNGC5,
242 CNGC6, and CNGC9, are required for constitutive growth of Arabidopsis root hairs as Ca²⁺-
243 permeable channels. *cell.com*YQ Tan, Y Yang, A Zhang, CF Fei, LL Gu, SJ Sun, W Xu, L Wang, H
244 Liu, YF WangPlant communications, 2020•cell.com
- 245 150. Tian L, Hires SA, Mao T, Huber D, Chiappe ME, et al. 2009. Imaging neural activity in worms,
246 flies and mice with improved GCaMP calcium indicators. *Nature Methods* 2009 6:12.
247 6(12):875–81
- 248 151. Tian W, Hou C, Ren Z, Wang C, Zhao F, et al. 2019. A calmodulin-gated calcium channel links
249 pathogen patterns to plant immunity. *Nature* 2019 572:7767. 572(7767):131–35
- 250 152. Toyota M, Spencer D, Sawai-Toyota S, Jiaqi W, Zhang T, et al. 2018. Glutamate triggers long-
251 distance, calcium-based plant defense signaling. *Science (1979)*. 361(6407):1112–15
- 252 153. Ugalde JM, Fuchs P, Nietzel T, Cutolo EA, Homagk M, et al. 2021. Chloroplast-derived photo-
253 oxidative stress causes changes in H₂O₂ and EGSH in other subcellular compartments. *Plant*
254 *Physiol*. 186(1):125–41
- 255 154. Ugalde JM, SchlöBer M, Dongois A, Martinière A, Meyer AJ. 2021. The latest HyPe(r) in plant
256 H₂O₂ biosensing. *Plant Physiol*. 187(2):480–84
- 257 155. Ulmasov T, Murfett J, Hagen G, Guilfoyle TJ. 1997. Aux/IAA proteins repress expression of
258 reporter genes containing natural and highly active synthetic auxin response elements. *Plant*
259 *Cell*. 9(11):1963–71

- 260 156. Ursache R, Andersen TG, Marhavý P, Geldner N. 2018. A protocol for combining fluorescent
261 proteins with histological stains for diverse cell wall components. *Plant J.* 93(2):399–412
- 262 157. Voon CP, Guan X, Sun Y, Sahu A, Chan MN, et al. 2018. ATP compartmentation in plastids and
263 cytosol of *Arabidopsis thaliana* revealed by fluorescent protein sensing. *Proc Natl Acad Sci U S*
264 *A.* 115(45):E10778–87
- 265 158. Waadt R, Hitomi K, Nishimura N, Hitomi C, Adams SR, et al. 2014. FRET-based reporters for the
266 direct visualization of abscisic acid concentration changes and distribution in *Arabidopsis*.
267 *Elife.* 3:e01739
- 268 159. Waadt R, Köster P, Andrés Z, Waadt C, Bradamante G, et al. 2020. Dual-reporting
269 transcriptionally linked genetically encoded fluorescent indicators resolve the spatiotemporal
270 coordination of cytosolic abscisic acid and second messenger dynamics in *Arabidopsis*. *Plant*
271 *Cell.* 32(8):2582–2601
- 272 160. Waadt R, Krebs M, Kudla J, Schumacher K. 2017. Multiparameter imaging of calcium and
273 abscisic acid and high-resolution quantitative calcium measurements using R-GECO1-
274 mTurquoise in *Arabidopsis*. *New Phytologist.* 216(1):303–20
- 275 161. Walia A, Waadt R, Jones AM. 2018. Genetically Encoded Biosensors in Plants: Pathways to
276 Discovery. *Annu Rev Plant Biol.* 69(1):497–524
- 277 162. Wang FL, Tan YL, Wallrad L, Du XQ, Eickelkamp A, et al. 2021. A potassium-sensing niche in
278 *Arabidopsis* roots orchestrates signaling and adaptation responses to maintain nutrient
279 homeostasis. *Dev Cell.* 56(6):781-794.e6
- 280 163. Whalley HJ, Knight MR. 2013. Calcium signatures are decoded by plants to give specific gene
281 responses. *New Phytologist.* 197(3):690–93
- 282 164. Wu R, Duan L, Pruneda-Paz JL, Oh DH, Pound M, et al. 2018. The 6xABRE synthetic promoter
283 enables the spatiotemporal analysis of ABA-mediated transcriptional regulation. *Plant Physiol.*
284 177(4):1650–65
- 285 165. Wu S-Y, Wen Y, Bernard N, Serre C, Charlotte C, et al. 2021. A sensitive and specific genetically
286 encodable biosensor for potassium ions. *bioRxiv.* 2021.10.07.463410
- 287 166. Xu SL, Shrestha R, Karunadasa SS, Xie PQ. 2023. Proximity Labeling in Plants. *Annu Rev Plant*
288 *Biol.* 74(Volume 74, 2023):285–312
- 289 167. Yang X, Zhang Q, Zhang S, Lai M, Ji X, et al. 2023. Molecule fluorescent probes for sensing and
290 imaging analytes in plants: Developments and challenges. *Coord Chem Rev.* 487:215154
- 291 168. Young JJ, Mehta S, Israelsson M, Godoski J, Grill E, Schroeder JI. 2006. CO₂ signaling in guard
292 cells: Calcium sensitivity response modulation, a Ca²⁺-independent phase, and CO₂
293 insensitivity of the *gca2* mutant. *Proc Natl Acad Sci U S A.* 103(19):7506–11
- 294 169. Yuan F, Yang H, Xue Y, Kong D, Ye R, et al. 2014. OSCA1 mediates osmotic-stress-evoked Ca²⁺
295 increases vital for osmosensing in *Arabidopsis*. *Nature* 2014 514:7522. 514(7522):367–71
- 296 170. Zhang L, Takahashi Y, Hsu PK, Kollist H, Merilo E, et al. 2020. FRET kinase sensor development
297 reveals SnRK2/OST1 activation by ABA but not by MeJA and high CO₂ during stomatal closure.
298 *Elife.* 9:1–74
- 299 171. Zhang S, Daniels DA, Ivanov S, Jurgensen L, Müller LM, et al. 2022. A genetically encoded
300 biosensor reveals spatiotemporal variation in cellular phosphate content in *Brachypodium*
301 *distachyon* mycorrhizal roots. *New Phytologist.* 234(5):1817–31
- 302 172. Zhang S, Pan Y, Tian W, Dong M, Zhu H, et al. 2017. *Arabidopsis* CNGC14 mediates calcium
303 influx required for tip growth in root hairs. *cell.com* Zhang, Y Pan, W Tian, M Dong, H Zhu, S
304 Luan, L Li *Molecular Plant, 2017*•*cell.com*
- 305 173. Zhang Y, Anfang M, Rowe J, Rizza A, Bar H, et al. 2024. ABA importers ABCG17 and ABCG18
306 redundantly regulate seed size in *Arabidopsis*. *Plant Commun*
- 307 174. Zhou S, Zhou J, Pan Y, Wu Q, Ping J. 2024. Wearable electrochemical sensors for plant small-
308 molecule detection. *Trends Plant Sci.* 29(2):219–31
- 309